

AVP-induced increase in AQP2 and p-AQP2 is blunted in heart failure during cardiac remodeling and is associated with decreased AT1R abundance in rat kidney

Lütken, Sophie Constantin; Frøkiær, Jørgen; Nielsen, Søren

Published in:
PLOS ONE

DOI (link to publication from Publisher):
[10.1371/journal.pone.0116501](https://doi.org/10.1371/journal.pone.0116501)

Publication date:
2015

Document Version
Publisher's PDF, also known as Version of record

[Link to publication from Aalborg University](#)

Citation for published version (APA):

Lütken, S. C., Frøkiær, J., & Nielsen, S. (2015). AVP-induced increase in AQP2 and p-AQP2 is blunted in heart failure during cardiac remodeling and is associated with decreased AT1R abundance in rat kidney. *PLOS ONE*, 10(2), Article 0116501. <https://doi.org/10.1371/journal.pone.0116501>

General rights

Copyright and moral rights for the publications made accessible in the public portal are retained by the authors and/or other copyright owners and it is a condition of accessing publications that users recognise and abide by the legal requirements associated with these rights.

- Users may download and print one copy of any publication from the public portal for the purpose of private study or research.
- You may not further distribute the material or use it for any profit-making activity or commercial gain
- You may freely distribute the URL identifying the publication in the public portal -

Take down policy

If you believe that this document breaches copyright please contact us at vbn@aub.aau.dk providing details, and we will remove access to the work immediately and investigate your claim.

RESEARCH ARTICLE

AVP-Induced Increase in AQP2 and p-AQP2 Is Blunted in Heart Failure during Cardiac Remodeling and Is Associated with Decreased AT1R Abundance in Rat Kidney

Sophie Constantin Lütken^{1,2*}, Jørgen Frøkiær², Søren Nielsen^{1,3}

1 Department of Biomedicine -Anatomy, University of Aarhus, DK-8000 Aarhus C, Denmark, **2** Institute of Clinical Medicine, Aarhus University Hospital, DK-8200 Aarhus N, Denmark, **3** Department of Health Science and Technology, Aalborg University, DK-9220 Aalborg Ø, Denmark

* sche@ana.au.dk



OPEN ACCESS

Citation: Lütken SC, Frøkiær J, Nielsen S (2015) AVP-Induced Increase in AQP2 and p-AQP2 Is Blunted in Heart Failure during Cardiac Remodeling and Is Associated with Decreased AT1R Abundance in Rat Kidney. PLoS ONE 10(2): e0116501. doi:10.1371/journal.pone.0116501

Academic Editor: Jeff M Sands, Emory University, UNITED STATES

Received: March 10, 2014

Accepted: December 10, 2014

Published: February 6, 2015

Copyright: © 2015 Lütken et al. This is an open access article distributed under the terms of the [Creative Commons Attribution License](https://creativecommons.org/licenses/by/4.0/), which permits unrestricted use, distribution, and reproduction in any medium, provided the original author and source are credited.

Funding: Support for this study was provided by the Karen Elise Jensen Foundation (www.kejfond.dk), Aase and Ejnar Danielsen Foundation (www.danielsensfond.dk), The Danish Heart Foundation (www.hjerteforeningen.dk), Carl and Ellen Hertz Foundation (poulroepstorff@mail.dk), The A.P. McKinney Møller Foundation for Medical Scientific Promotion (www.apmollerfonde.dk), Human Frontier Science Program, the European Commission (QRLT 2000 00778 and QRLT 2000 00987) (www.hfsp.org), and the intramural budget of the National Heart, Lung, and Blood Institute, National Institutes of Health

Abstract

Aim

The objective was to examine the renal effects of long-term increased angiotensin II and vasopressin plasma levels in early-stage heart failure (HF). We investigated the regulations of the V2 vasopressin receptor, the type 1A angiotensin II receptor, the (pro)renin receptor, and the water channels AQP2, AQP1, AQP3, and AQP4 in the inner medulla of rat kidney.

Methods

HF was induced by coronary artery ligation. Sixty-eight rats were allocated to six groups: Sham (N = 11), HF (N = 11), sodium restricted sham (N = 11), sodium restricted HF (N = 11), sodium restricted sham + DDAVP (N = 12), and sodium restricted HF + DDAVP (N = 12). 1-desamino-8-D-arginine vasopressin (0.5 ng h⁻¹ for 7 days) or vehicle was administered. Pre- and post-treatment echocardiographic evaluation was performed. The rats were sacrificed at day 17 after surgery, before cardiac remodeling in rat is known to be completed.

Results

HF rats on standard sodium diet and sodium restriction displayed biochemical markers of HF. These rats developed hyponatremia, hypo-osmolality, and decreased fractional excretion of sodium. Increase of AQP2 and p(Ser256)-AQP2 abundance in all HF groups was blunted compared with control groups even when infused with DDAVP and despite increased vasopressin V2 receptor and Gsα abundance. This was associated with decreased protein abundance of the AT1A receptor in HF groups vs. controls.

Conclusion

Early-stage HF is associated with blunted increase in AQP2 and p(Ser256)-AQP2 despite of hyponatremia, hypo-osmolality, and increased inner medullary vasopressin V2 receptor

(www.nhlbi.nih.gov). The funders had no role in study design, data collection and analysis, decision to publish, or preparation of the manuscript. The authors confirm that there are no restrictions on sharing of data and/or materials from any funders or organisations listed above.

Competing Interests: The authors have read the journal's policy and have the following conflicts: Jørgen Frøkiær is vice president of the Danish Council for Independent Research. The authors have received research funding from the following organisations: Karen Elise Jensen Foundation, Aase and Ejnar Danielsen Foundation, Danish Council for Independent Research, The Novo Nordisk Foundation, The Danish Heart Foundation, Carl and Ellen Hertz Foundation, The A.P. Mc-Kinney Møller Foundation for Medical Scientific Promotion, Human Frontier Science Program, the European Commission (QRLT 2000 00778 and QRLT 2000 00987), and the intramural budget of the National Heart, Lung, and Blood Institute, National Institutes of Health. The authors confirm that this does not alter their adherence to PLOS ONE policies on sharing data and materials.

expression. Decreased type 1A angiotensin II receptor abundance likely plays a role in the transduction of these effects.

Introduction

Heart failure (HF) is associated with activation of the renin-angiotensin system (RAS) and sustained increased vasopressin (AVP) release from the pituitary gland [1–5]. RAS and AVP have been shown to play a role in the kidneys by taking part in the development of hyponatremia and water retention. Hyponatremia and water retention in HF is associated with a poor outcome [6,7]. There is increasing evidence of a crosstalk between angiotensin II (ANG II) and AVP with potential enhancing effects on water retention mediated by renal water channels [8–10]. We have previously demonstrated that rats with chronic HF 21 days after myocardial infarction (MI) increased the abundance of the renal water channel aquaporin-2 (AQP2) in the inner medullary collecting ducts (IMCDs) [11]. When treated with the type 1_A angiotensin II receptor (AT1R) blocker candesartan, HF rats down regulated IMCD AQP2 expression to sham levels [9]. This supports that a crosstalk between the V2 vasopressin receptor (V2R) and AT1R is possible and potentially important in AQP2 regulation. In contrast, the constitutively expressed AQP1 including the basolateral aquaporins AQP3 and AQP4 remained unchanged both in rats after water loading and in HF rats [11–13].

HF is a progressive condition with short- and long-term adaptations to maintain blood pressure and perfusion to vital organs. Previous HF studies focused on water retention in the stable intermediate stage of HF after 21 days in the rat, when cardiac remodeling has been completed [14–16]. Even though diuretics play a crucial role in standard HF treatment, the subcellular basis for the development of water retention has not previously been investigated in the early stage after MI, a period of clinical interest due to the increased risk of arrhythmias and death [17]. Furthermore, the complexity of HF makes it difficult to distinguish between the various actions of key hormones in HF development. As HF is an evolving condition, one could speculate whether initial and potential beneficial adaptations are abolished in later stages of disease.

Low-sodium diet is a well-known method to increase endogenous ANG II levels. In co-treatment with infusions of the selective V2-receptor (V2R) agonist 1-desamino-8-D-arginine vasopressin (DDAVP), low-sodium diet has been used in rat models to study renal changes in water retention [8,18]. To our knowledge these models have never been directly compared with or applied to a HF model. Thus, the aim of the present study was to 1) investigate whether the inner medullary changes to low-sodium diet and DDAVP infusion in controls are comparable with the changes seen in early-stage HF. 2) Investigate the renal effects of clamped ANG II levels in early-stage HF in combination with DDAVP. 3) to investigate whether IM expressions of AQP2, p-AQP2 and AQP1, AQP3, and AQP4 in early-stage HF are changed compared with healthy animals under basic states and in conditions with enhanced ANG II levels and DDAVP infusion, and 4) to examine whether these changes are associated with changes in cardiac function, V2R, AT1R and the (pro)renin receptor (P)RR.

Methods

Experimental animals

Sixty-eight male Munich-Wistar rats obtained from Harlan Laboratories, Denmark with an initial weight of 250 g were initially given free access to tap water and standard rat chow (Altromin 1324, Altromin, Lage, Germany). The rats were housed under controlled temperature

($21 \pm 2^\circ\text{C}$) and humidity ($55 \pm 2\%$) in a 12:12-h light-dark cycle and acclimatized for 7 days before surgery. All animal protocols were approved by the board at the Institute of Clinical Medicine, University of Aarhus according to the licenses for use of experimental animal issued by the Danish Ministry of Justice.

Animal preparations

HF was induced by free wall MI following ligation of the left anterior descending artery (LAD) as previously described in detail [9]. Sham operated animals underwent the same procedure, without ligation of the LAD. Buprenorphine (0.12 mg/kg sc; Anorfin, GEA, Frederiksberg, Denmark) was administered twice for 2 days to relieve postoperative pain. The rats were kept in a 100% oxygen environment for 24 h after surgery. With this method mortality rate was 15% in rats that underwent LAD ligation.

Study design

As shown in Fig. 1, sham operation or ligation of the LAD was performed day zero (Sham rats, $N = 34$; HF, $N = 34$). For increasing survival rate, the animals were allowed to recover the surgical procedure for ten days. At day ten the two groups were subdivided into six groups as described in the following. After echocardiographic evaluation, the rats were allocated into two diet types. Either standard diet (Altromin 1324, Altromin, Lage, Germany) containing 0.2% sodium (Sham rats, $N = 11$; HF, $N = 11$), or low sodium diet (Altromin C1036) containing 0.015% sodium (L-Sham, $N = 23$; L-HF, $N = 23$). Estimated daily sodium intake in the animals receiving low sodium diet was $0.60 \text{ meq Na}^+ \cdot (250\text{g BW})^{-1} \cdot \text{day}^{-1}$. The rats receiving low sodium diet were further subdivided. Thus, half of the rats on low sodium diet received DDAVP infusion (V1005, Sigma, $0.5 \text{ ng} \cdot \text{h}^{-1}$) dissolved in physiological saline for 7 days administered via osmotic minipumps (Alzet mini-osmotic pumps model 2201, Scanbur, K ge, Denmark), as previously described (L-Sham, $N = 11$; L-HF, $N = 11$ and L-Sham+d, $N = 12$; L-HF+d, $N = 12$) [8]. All rats not receiving DDAVP were treated with vehicle only. All groups were matched according to ejection fraction (EF) and weight and had free access to tap water during the entire experiment. The animals were placed individually in metabolic cages (Scanbur, K ge, Denmark) for the last seven days of the experiment to allow clearance studies. After seven days of DDAVP infusion and seventeen days after MI, the rats were sacrificed and the kidneys were rapidly removed and processed for membrane fraction and immunoblotting the same day.

Echocardiographic evaluation

Day ten and sixteen in experiment echocardiographic evaluation was performed. Transthoracic echocardiography was obtained with Vivid7 Ultrasound Scanner (GE Medical Systems) using a 10S transducer (11.5 MHz). The echocardiographic scanner was kindly provided by Professor Erik Sloth, Department of Anaesthesia and Intensive Care, Aarhus University Hospital –Skejby, Denmark. All images and subsequent measurements were performed according to American Society of Echocardiography (ASE) guidelines [19,20]. The rats were lightly anesthetized with 1–2% isoflurane and 100% oxygen, their chest shaved and cleaned with alcohol, and electrode pads with ECG electrodes were gently placed with sleek tape on both forepaws and left hindpaw. Penetration depth was 2 cm, width was as small as possible, and frames per second were set on maximal. The rats were positioned on their left side with the transducer placed on the left hemithorax. Care was taken to avoid pressure on the thorax potentially causing bradycardia and alteration of cardiac filling. Two-dimensional images and M-mode tracings of the parasternal short-axis view at the level of the papillary muscles and apical four-chamber view were obtained. It was ensured that the image was on axis based on

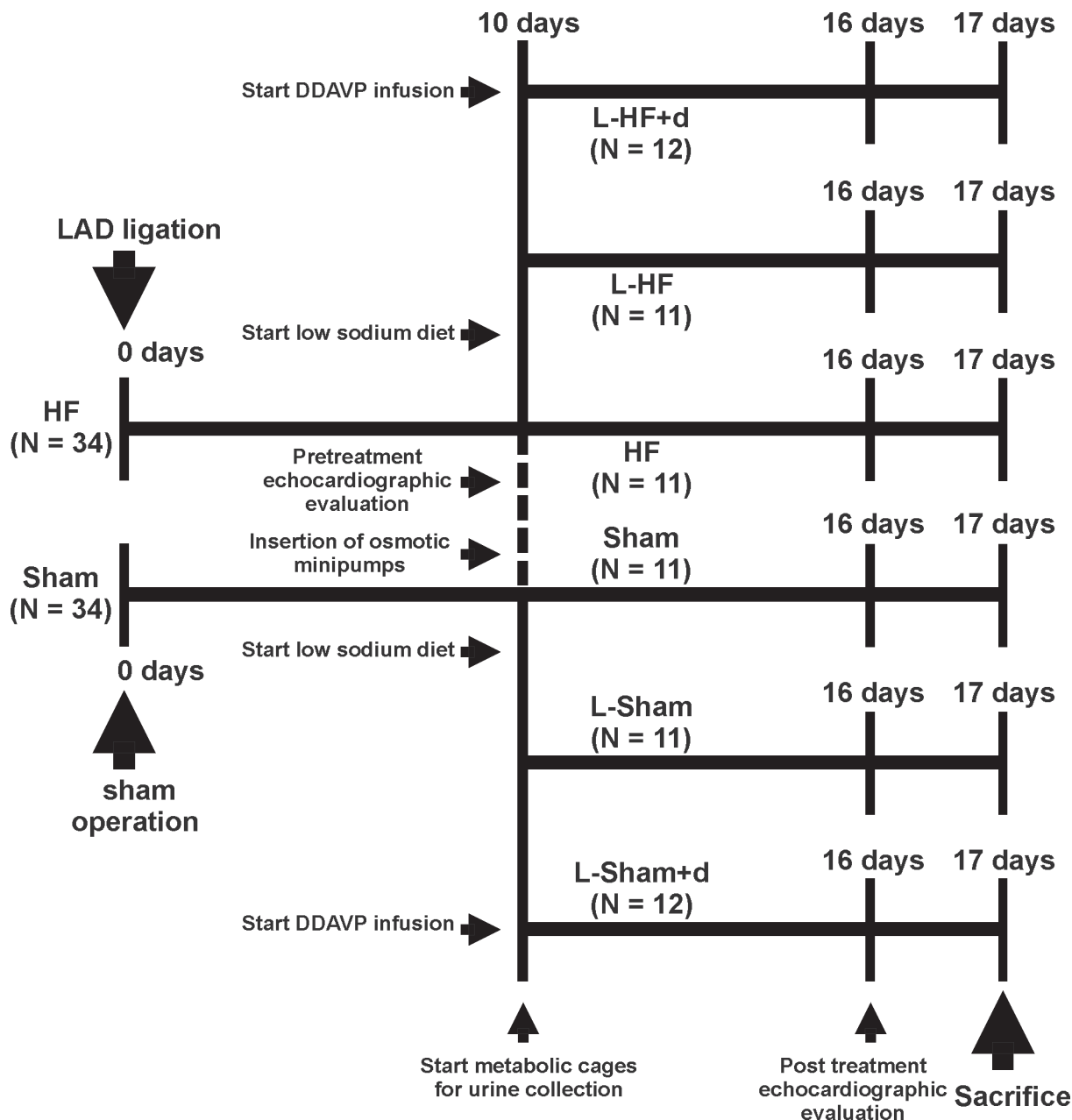


Fig 1. Diagram of study design. Sham operation or ligation of the left anterior descending artery (LAD) was performed day 0. Day 10: The rats underwent echocardiographic evaluation before allocation to standard diet or low sodium diet. Half of the rats on low sodium diet also received DDAVP infusion in osmotic minipumps for 7 days. The rats were maintained in metabolic cages over the last 7 days for clearance studies. At day 16, post-treatment echocardiographic evaluation was performed. Day 17 the rats were sacrificed and the kidneys processed for membrane fractionation and immunoblotting the same day.

doi:10.1371/journal.pone.0116501.g001

roundness of the left ventricular cavity at the level of the papillary muscles. The time of end-diastole was defined as the maximal diameter of the left ventricle (LV). Accordingly, end-systole was defined as the minimal diameter in the same heart cycle. At least three heart cycles were averaged for each measurement. All measurements were performed manually. Data were analyzed using Echopac PC (GE Medical Systems). Left ventricular end-diastolic and end-systolic volumes (LVEDV and LVESV, respectively) were calculated from LV diastolic (LVDA) and LV systolic (LVSA) areas via the bullet equation [21,22]. Ejection

fractions (EF) were calculated from diastolic and systolic volumes as $[(LVEDV - LVESV) / LVEDV \cdot 100]$. Heart rate (HR) was calculated from beats per second obtained by pulse wave Doppler mitral inflow measurements from the apical four-chamber view during ten seconds due to the fast heart rate in small animals. Sample volume was set at the highest size available during this particular recording. HR as beats per minute (BPM) was calculated as $[\text{number of systolic mitral inflows} \cdot 60]$. Inclusion criteria for the rats that underwent LAD-ligation was $EF < 50\%$ at day ten in experiment.

Clearance studies

Before euthanasia, 6–8 ml of blood was collected into a heparinized tube for determination of plasma electrolytes and osmolality. For clearance studies, urine samples were immediately stored at -20°C . Plasma concentrations of sodium and potassium were determined on the last day of experiment (Vitros 950, Johnson & Johnson). The concentrations of urinary sodium and potassium were determined by standard flame photometry (Eppendorf FCM6341). The urine and plasma osmolality was measured with a vapor pressure osmometer (Osmomat 030, Gonotec, Berlin, Germany). From the obtained measurements, electrolyte free water reabsorption ($T^{\text{c}}\text{H}_2\text{O}$) was calculated as:

$$T^{\text{c}}\text{H}_2\text{O} = \text{UO} \cdot \left(\frac{\text{UNa} + \text{UK}}{\text{PNa}} - 1 \right)$$

Where $T^{\text{c}}\text{H}_2\text{O}$ is electrolyte free water reabsorption, UO is daily urinary flow rate, UNa is urine sodium, UK is urine potassium, and PNa is plasma sodium [23–25].

Immunohistochemistry

After rapid anesthesia with 3% isoflurane, the left kidneys were fixed by retrograde perfusion via the aorta with 3% paraformaldehyde in 0.01 M PBS, pH 7.4. Briefly, the kidney was removed, and the midregion was sectioned into 2- to 3-mm transverse sections and immersion fixed for an additional 1 h, followed by three 10-min washes with 0.01 M PBS buffer, pH 7.4. The tissue was dehydrated in graded ethanol and left overnight in xylene. Paraffin-embedded sections (2 μm thickness) were cut on a rotary microtome (Leica Microsystems, Herlev, Denmark). Immunolabeling with AQP2 and p-AQP2 was performed on sections from the paraffin-embedded preparation using methods described previously in detail [9,26].

Semiquantitative immunoblotting

The right kidney was quickly removed and inner medulla (IM) dissected from the remaining kidney. IM from each rat was individually homogenized (Ultra-Turrax T8 homogenizer, IKA Labortechnik, Staufen, Germany) in ice-cold isolation solution containing 0.3 M sucrose, 25 mM imidazole, and 1 mM EDTA, pH 7.2, the protease inhibitors 8.5 μM leupeptin (Sigma-Aldrich) and 0.4 mM Pefabloc (Roche) and the phosphatase inhibitors sodium orthovanadate (0.0184 g/100 ml buffer; Sigma-Aldrich), sodium fluoride (0.1052 g/100 ml buffer; Merck, Whitehouse Station, NJ), and okadaic acid (16.4 μl /100 ml buffer; Calbiochem, San Diego, CA). The homogenates were then centrifuged at 1000 g for 15 min at 4°C to remove whole cells, nuclei, and mitochondria, and gel samples were prepared from the supernatant in Laemmli sample buffer containing 2% SDS and dithiothreitol and solubilized at 65°C , and stored at -20°C . The total protein concentration of the homogenate was measured using a Pierce BCA protein assay kit (Roche, Basel, Switzerland). Samples of membrane fractions were run on polyacrylamide gels (Criterion TGX Long Shelf Life Precast Gels, Any kD, Bio-Rad

Laboratories Inc., USA). To ascertain identical loading and to allow for correction, an identical gel was run in parallel and subjected to Coomassie Brilliant Blue staining, as previously described in detail [9,27]. SDS-PAGE was performed on polyacrylamide gels (Criterion TGX Long Shelf Life Precast Gels, Any kD and Criterion TGX Precast Gels 4–15%, Bio-Rad Laboratories Inc., USA). Each lane was loaded with ~12 µg of protein from samples from a different rat.

The proteins from kidney IM were transferred to a polyvinylidene difluoride (PVDF) membrane (Immobilon-P PVDF Transfer Membrane, Millipore, Cat. No. IPVH 00010) using the BioRad Trans-Blot Turbo Transfer System with an ice-cold transfer buffer containing 200 ml 5 x Bio-Rad Trans-Blot Turbo Transfer Buffer mixed with 600 ml nanopure water and 200 ml 92% ethanol. The blots were blocked with 5% nonfat dry milk in PBS-T (80 mM Na₂HPO₄, 20 mM NaH₂PO₄, 100 mM NaCl, 0.1% Tween 20, adjusted to pH 7.4 with 10 M NaOH) or by using a blocking buffer containing 50% 0.1M PBS and 50% Odyssey Infrared Imaging System Blocking Buffer (LI-COR Biosciences, Cambridge, UK). After washing with PBS-T, the blots were incubated with primary antibodies overnight at 4°C on a tilting table. The antigen-antibody complex was visualized with horseradish peroxidase (HRP)-conjugated secondary antibodies (P447 or P448, diluted 1:3000, Dako) using the ECL system (Amersham Pharmacia Biotech) or visualized with LI-COR IRDye-conjugated secondary antibodies (IRDye 926-32213 and 926-32212 in the 700 and 800 nm channel, diluted 1:12000, LI-COR Biosciences, Cambridge, UK). Odyssey Infrared Imager (LI-COR Biosciences, Cambridge, UK) connected to a computer running Odyssey v. 12 was used for visualization. ECL films were digitalized using an Epson Perfection 2450 scanner and all band densities were quantified by using ImageJ [28]. The specific bands were corrected to the Coomassie gels and normalized to the mean of control bands.

Primary antibodies

For semiquantitative immunoblotting, we used previously characterized monoclonal and polyclonal antibodies as summarized below.

AQP2 (H7661), an affinity-purified rabbit polyclonal antibody raised against AQP2 has previously been described [29].

pS256-AQP2 (KO307), an affinity-purified rabbit polyclonal antibody raised against pS256-AQP2 has previously been described [30,31].

V2R (7251 AP): an affinity-purified rabbit polyclonal antibody raised against V2R has previously been described [32].

AQP3 (1591AP): an affinity-purified rabbit polyclonal antibody raised against AQP3 has previously been described [33,34].

AQP1 (2353 AP fr. 2–5): an affinity-purified rabbit polyclonal antibody raised against AQP1 has previously been described [35].

Na-K-ATPase α1-subunit 3B: an affinity-purified mouse monoclonal antibody raised against the Na-K-ATPase α1-subunit has previously been described [26,36].

The following commercial antibodies used in this study are summarized below.

AQP4 GST fusion peptide (Alomone labs, Jerusalem, Israel)

Heteromeric G protein subunit Gsα 371732 (Calbiochem-Novabiochem, San Diego, CA)

AT1 receptor (sc-579 rabbit polyclonal, Santa Cruz Biotechnology Inc.)

ATP6AP2 Renin receptor (ab40790, AbCam, Cambridge, UK)

Grouping on gels

According to focus, all antibodies were incubated on gels containing the following combination of groups:

1. The regulation of early-stage HF on standard diet vs. enhanced RAS controls. Groups: Sham (n = 7); HF (n = 6); L-Sham (n = 8).
2. The regulation of early-stage HF with enhanced RAS vs. RAS enhanced controls. Groups: Sham (n = 7); L-HF (n = 7); L-Sham (n = 8).
3. The difference in regulation of standard diet HF, RAS enhanced HF, and RAS enhanced HF with DDAVP clamping. Groups: HF (n = 6); L-HF+d (n = 8); L-HF (n = 7).
4. The regulation of RAS enhanced HF and DDAVP clamping vs. RAS enhancement and DDAVP clamping in controls vs. RAS enhanced controls. Groups: L-Sham (n = 8); L-HF+d (n = 8); L-Sham+d (n = 8).
5. The regulation of RAS enhanced controls with DDAVP clamping vs. standard diet controls and RAS enhanced controls. Baseline conditions in healthy sham operated rats were thereby revealed during diet change and pharmacological interventions. Groups: Sham (n = 7); L-Sham+d (n = 8); L-Sham (n = 8).

Statistical analysis

Data are expressed as means \pm SE. Statistical significance between groups was estimated with one-way analysis of variance (ANOVA) followed by the Tukey-Kramer method for unequal sample sizes to test all possible pairwise differences of means to determine whether at least one difference was significantly different from 0. When assumptions for ANOVA were not fulfilled, Kruskal-Wallis nonparametric test was performed. *P* values < 0.05 were considered significant.

Results

Echocardiographic analysis

Data are presented in Tables 1 and 2. Table 1 displays the baseline echocardiographic findings day ten, retrieved before the allocation of the supplemental subgroups. At baseline all echocardiographic parameters changed in HF rats except heart rate with significant loss of cardiac function shown by ejection fraction (EF). EF was decreased from $70 \pm 1\%$ in Sham animals to $41 \pm 1\%$ in HF.

The rats were re-examined after another six days, shown in Table 2. All HF groups exhibited significant decreased EF and increased heart rate vs. Sham. No difference in EF among HF groups was observed. In contrast, L-Sham and L-Sham+d increased EF compared with Sham rats. These findings altogether indicated progression of cardiac disease not only in all HF groups but also in both sodium restricted sham groups.

Clearance studies

Data are presented in Table 3. Mean body weight was unchanged among groups, and did not differ at any time in the study period (data not shown). Plasma osmolality was significantly decreased in all groups, including standard diet HF rats compared with sham rats 17 days after MI. L-HF developed the largest decline in plasma osmolality, whereas L-Sham+d and L-HF+d were comparable. Urine-to-plasma osmolality ratio increased in all sodium restricted groups except L-HF. Plasma urea was significantly increased in L-HF vs. L-Sham, and in L-HF+d vs. L-Sham+d. Urine urea increased in L-Sham, L-Sham+d, and L-HF+d, respectively. Electrolyte free water reabsorption takes the amount of urea in urine and plasma into account. Electrolyte free water reabsorption ($T^c\text{CH}_2\text{O}$) was expectedly decreased in all sodium restricted groups, but

Table 1. Pretreatment echocardiographic parameters.

	Sham	HF
n	34	34
EF, %	70 ± 1	41 ± 1*
HR, bpm	321 ± 4	315 ± 4

Values are expressed as means ± SE. These values were measured at day 10 in the experiment, i.e. 10 days after MI surgery. *n*, number of rats;

EF;

left ventricular ejection fraction HR, heart rate;

**P* < 0.001 vs. Sham.

doi:10.1371/journal.pone.0116501.t001

was slightly increased in the two DDAVP groups vs. L-Sham. Consistently, DDAVP groups decreased urine output on the last day of monitoring compared with the other sodium restricted groups, despite of comparable water intake. HF rats exhibited decreased levels of fractional urinary excretion of sodium (FeNa) compared with sham rats in presence of unchanged creatinine clearance (Ccr), otherwise no difference among groups was observed. Urinary sodium excretion [urine sodium (UNa) x urine output (UO)] and urinary potassium excretion [urine sodium (UK) x urine output (UO)] were decreased in all sodium restricted groups compared with Sham and HF rats. Plasma sodium was significantly decreased in HF rats compared with Sham rats, and in L-HF and L-HF+d rats vs. L-Sham. Plasma potassium remained within standard range among groups. Substantial decreases in Ccr and plasma creatinine were observed in L-HF and L-HF+d compared with all control groups. Together with hyponatremia these results are consistent with cardiac decompensation.

Blunted increase of AQP2 and p(Ser256)-AQP2 abundance in all HF groups

Previously, we demonstrated that chronic HF 21 and 29 days after MI was associated with increased protein levels of AQP2 and p-AQP2 in IM. Semiquantitative immunoblotting was carried out to examine IM kidney abundance of AQP2 and p-AQP2. The purposes were: 1) to test whether changes in expression of AQPs play an important role in the early stages of HF before

Table 2. Post treatment echocardiographic parameters.

	Sham	HF	L-sham	L-HF	L-sham+d	L-HF+d
n	11	11	11	11	12	12
EF, %	66 ± 1	42 ± 2*	72 ± 2*#	41 ± 3*‡	70 ± 1*#‡♠	41 ± 2*‡♣
HR, bpm	326 ± 8	354 ± 5*	362 ± 7*	362 ± 6*	358 ± 4*	352 ± 8*‡

Values are expressed as means ± SE. These values were measured at day 16 in the experiment, i.e. 16 days after MI surgery. *n*, number of rats;

EF; left ventricular ejection fraction;

HR, heart rate; bpm, beats per minute.

**P* < 0.05 vs. Sham

P < 0.05 vs. HF

‡ *P* < 0.05 vs. L-Sham

♠ *P* < 0.05 vs. L-HF

♣ *P* < 0.05 vs. L-Sham+d.

doi:10.1371/journal.pone.0116501.t002

Table 3. Changes in renal function.

	Sham	HF	L-sham	L-HF	L-sham+d	L-HF+d
n	11	11	11	11	12	12
BW, g	363 ± 8	358 ± 7	360 ± 12	358 ± 6	354 ± 8	360 ± 6
Water intake, ml	32 ± 1	32 ± 1	18 ± 1*#	22 ± 1*#‡	17 ± 1*#	16 ± 1*#
UO, $\mu\text{l}\cdot\text{min}^{-1}\cdot\text{kg}^{-1}$	21.4 ± 1.8	24.5 ± 1.8	13.0 ± 1.3*#	15.5 ± 2.0*#	8.3 ± 0.9*#‡□	8.2 ± 1.2*#‡□
U-Osm, mosm/KgH ₂ O	2217 ± 113	2134 ± 131	2444 ± 180	2171 ± 183	3279 ± 73*#‡□	3273 ± 101*#‡□
P-Osm, mosm/KgH ₂ O	299 ± 1	296 ± 1*	287 ± 7*	245 ± 15*#‡	281 ± 4*#□	284 ± 4*#□
U/P-Osm	7.4 ± 0.4	7.4 ± 0.4	9.6 ± 0.6*#	7.6 ± 0.4#‡	11.3 ± 0.2*#‡□	11.1 ± 0.4*#‡□
P-Urea, mmol/l	7.9 ± 0.4	7.9 ± 0.2	6.4 ± 0.5*#	7.7 ± 0.3‡	7.5 ± 0.2‡	8.2 ± 0.2‡♣
U-Urea, mmol/l	1219 ± 58	1320 ± 164	1731 ± 155*#	1371 ± 168	2477 ± 111*#‡□	2394 ± 114*#‡□
T [°] cH ₂ O, $\mu\text{l}/\text{min}$	24.8 ± 3.3	23.0 ± 1.9	5.5 ± 0.6*#	6.2 ± 0.7*#	6.8 ± 1.0*#‡	7.0 ± 0.9*#‡
FeNa, %	0.643 ± 0.040	0.443 ± 0.037*	0.009 ± 0.002*#	0.010 ± 0.001*#	0.013 ± 0.003*#	0.010 ± 0.001*#
UNa x UO, mmol	1.38 ± 0.19	1.36 ± 0.11	0.03 ± 0.00*#	0.03 ± 0.01*#	0.04 ± 0.01*#	0.02 ± 0.00*#
UK x UO, mmol	4.9 ± 0.5	4.9 ± 0.3	2.0 ± 0.2*#	2.3 ± 0.2*#‡	1.9 ± 0.2*#	2.0 ± 0.3*#
P-Na, mmol/l	139 ± 1	136 ± 0*	137 ± 0*	134 ± 1*‡	136 ± 0*	130 ± 4*‡♣
P-K, mmol/l	5.0 ± 0.1	5.0 ± 0.1	4.8 ± 0.1*#	4.5 ± 0.2*#	4.3 ± 0.1*#‡	4.5 ± 0.1*#
P-Cr, $\mu\text{mol}/\text{l}$	44 ± 2	40 ± 1	36 ± 2*#	41 ± 1‡	38 ± 1*	37 ± 1*□
Ccr, ml/min	1.49 ± 0.08	1.50 ± 0.07	1.81 ± 0.17	1.18 ± 0.07*#‡	1.39 ± 0.05‡□	1.17 ± 0.09*#‡♣

Values are expressed as means ± SE. The plasma values are measured at the last day of experiment whereas urine values and body weights are measured the day before to avoid error due to anesthesia under echocardiographic measurements. n, number of rats;

BW, median body weight;

Water intake, water intake;

UO, urine output; U-Osm, urine osmolality;

P-Osm, plasma osmolality;

U/P Osm, urine-to-plasma osmolality ratio;

P-Urea, plasma urea;

U-Urea, urine urea;

T[°]cH₂O, electrolyte free water reabsorption;

FENa, fractional excretion of sodium into urine;

UNa x UO, rate of urinary sodium excretion;

UK x UO, rate of urinary potassium excretion;

P-Na, plasma sodium;

P-K, plasma potassium;

P-Cr, plasma creatinine;

Ccr, creatinine clearance.

**P* < 0.05 vs. Sham

P < 0.05 vs. HF

‡ *P* < 0.05 vs. L-Sham

□ *P* < 0.05 vs. L-HF

♣ *P* < 0.05 vs. L-Sham+d.

doi:10.1371/journal.pone.0116501.t003

cardiac remodeling is complete. 2) to test whether the changes in plasma sodium and osmolality could be, in part, explained by changes in IM aquaporin abundances. Immunoblots are presented in Fig. 2 and the corresponding data in Table 4. In contrast to our previous findings in HF rats 21 and 29 days after MI [9,11], there was no change in AQP2 and p-AQP2 protein levels when compared between Sham groups and HF groups 17 days after MI. Neither sodium restriction nor DDAVP infusion increased AQP2 and p-AQP2 abundance in HF (Fig. 2, A, B

and F, G). Indeed, the two sodium restricted HF groups revealed decreased AQP2 and p-AQP2 abundances vs. HF (Fig. 2, C and H). In contrast, AQP2 and p-AQP2 abundances were increased in L-Sham+d vs. L-Sham, as previously described (Fig. 2, D, E and I, J) [8].

Phosphorylation at the Ser256 site near the COOH terminal of the AQP2 molecule is necessary for hormone regulated shuttling of AQP2 to the apical plasma membrane [30,37]. On this background we wanted to test, whether the observed changes in total AQP2 were accompanied by similar changes in p-AQP2. The changes of IM p-AQP2 in Fig. 2, F–J were comparable with the changes observed in AQP2, except there were no statistically changes in p-AQP2 abundances between the L-HF+d and L-HF rats (Fig. 2, C and H).

AQP2 and p(Ser256)-AQP2 distribution remained unchanged in all HF groups

Additional immunocytochemistry was performed to investigate whether the observed changes in AQP2 and p-AQP2 by immunoblot were associated with changes in subcellular localization (Fig. 3, A – L). AQP2 and p-AQP2 demonstrated similar distribution and the findings were consistent with previous studies.

Intracellular and a minor amount of basal staining of AQP2 and p-AQP2 was observed in standard diet Sham from IMCD principal cells (Fig. 3, A and B) [38]. As shown previously, the AQP2 and p-AQP2 staining was observed mainly in the apical domains in HF rats (Fig. 3, G and H) [2,9,11]. L-Sham and L-Sham+d revealed similar distributions of AQP2 and p-AQP2 with mainly apical staining, (Fig. 3, C, D and E, F, respectively) [8]. In the HF groups a profound apical labeling with virtually no intracellular staining was observed. These changes in AQP2 and p-AQP2 distribution were similar between HF, L-HF, and L-HF+d, respectively (Fig. 3, G, H and I, J, and K, L).

V2 vasopressin receptor abundance in inner medulla is only increased in HF rats and L-HF rats

To examine whether the observed changes in AQP2 and p-AQP2 could be due to changes in V2R abundance, semiquantitative immunoblotting was carried out. Immunoblots are presented in Fig. 4 and the corresponding data in Table 5. HF rats increased V2R to L-Sham levels vs. Sham (Fig. 4, A). In contrast, L-HF did not significantly increase vs. Sham and L-Sham (Fig. 4, B). No change between L-Sham, L-Sham+d, and L-HF+d was observed, but L-Sham and L-Sham+d increased V2R abundance vs. standard diet Sham (Fig. 4, D and E). In contrast, L-HF+d decreased V2R abundance vs. HF and L-HF rats (Fig. 4, C).

The Gs α subunit is increased in HF and L-HF rats but not in L-HF+d

To investigate whether the observed changes in V2R abundance were associated with concomitant changes in the associated protein G coupled pathway, semiquantitative immunoblotting was carried out. Immunoblots are presented in Fig. 5 and the corresponding data in Table 6. IM Gs α protein abundance was increased in HF and L-HF vs. Sham and L-Sham (Fig. 5, A and B). A similar increase was observed in L-Sham+d (Fig. 5, E). In contrast, L-HF+d remained comparable with L-Sham (Fig. 5, D).

The type-1 angiotensin II receptor is downregulated in HF and L-HF+d

Previous studies have indicated a possible crosstalk between the V2R and the AT1R, which could be important in the pathophysiology of early-stage HF 17 days after MI [8,9]. Low sodium diet with normal levels of potassium stimulates the endogenous production of ANG II

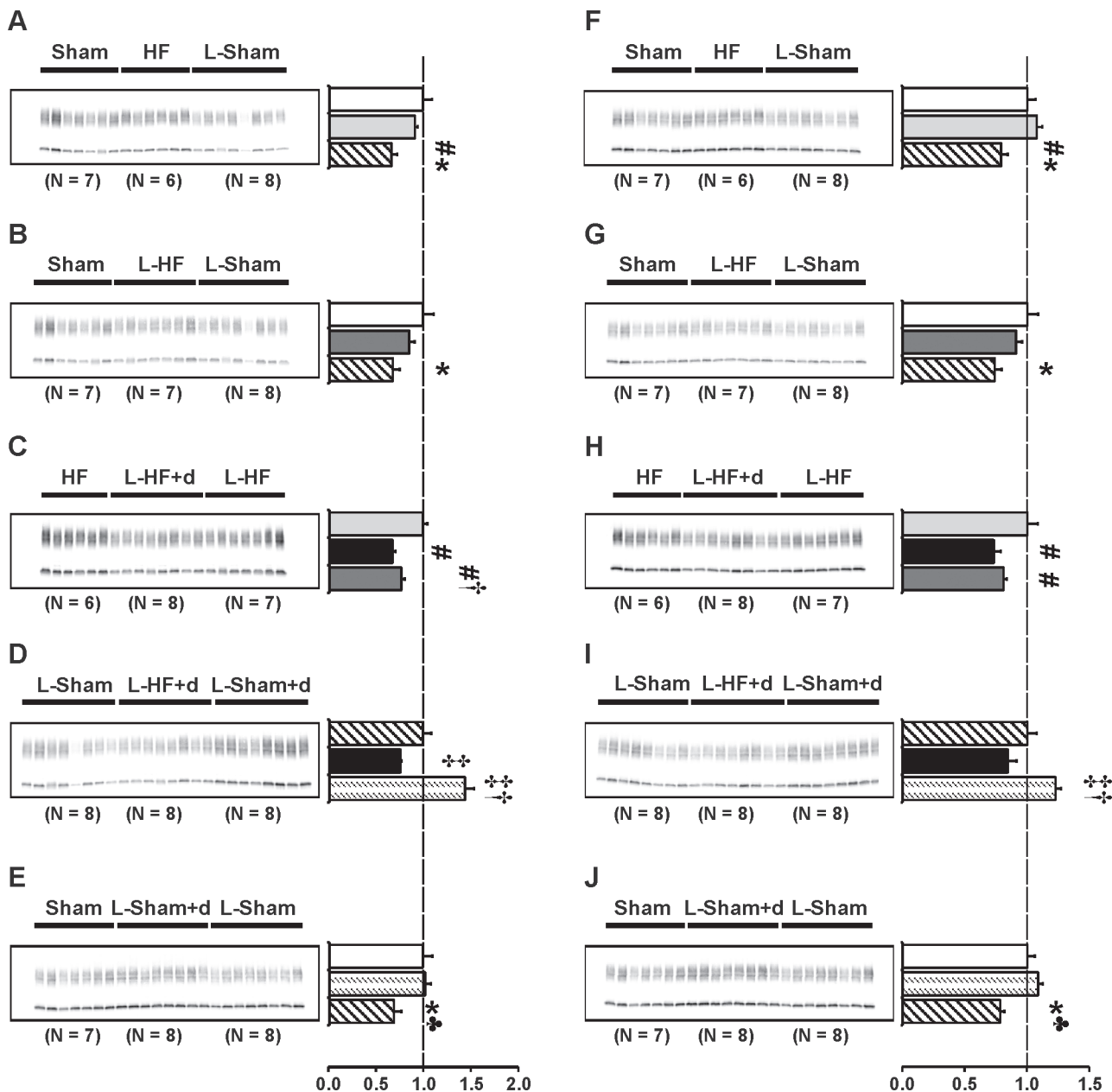


Fig 2. AQP2 and p-AQP2 abundance. Semiquantitative immunoblotting of kidney protein prepared from inner medulla. Immunoblot was reacted with anti-AQP2 (A-E) and AQP2 phosphorylated at Ser256 (p-AQP2) (F-J) antibody. Both antibodies reveal specific 29 kDa and 35–50 kDa bands. Data are presented in Table 4. Densitometric analysis revealed unchanged AQP2 and p-AQP2 protein levels in HF and L-HF vs. Sham 17 days after MI. Neither sodium restriction nor DDAVP infusion increased AQP2 and p-AQP2 abundance in HF as otherwise observed in L-Sham+d (A, B and F, G). Consistently, L-HF+d revealed decreased AQP2 and p-AQP2 abundance to L-HF levels vs. L-Sham and HF (C, D and H, I). Furthermore, AQP2 and p-AQP2 expression was decreased in L-Sham rats compared with Sham, HF, and L-Sham+d (A, B, E and F, G, J, respectively). In contrast, no difference was observed in L-Sham+d was observed vs. Sham (E and J). Each column represents the mean ± SE. Each column represents the mean ± SE. Solid white, Sham; solid light grey, HF; line pattern, L-Sham; solid dark grey, L-HF; solid black, L-HF+d; dotted pattern, L-Sham+d. **P* < 0.05 vs. Sham, #*P* < 0.05 vs. HF, †*P* < 0.05 vs. L-HF+d, ‡*P* < 0.05 vs. L-Sham, ♣*P* < 0.05 vs. L-Sham+d.

doi:10.1371/journal.pone.0116501.g002

whereas ALDO levels are kept near baseline [8]. Thus we examined whether the observed changes of AQP2 and p-AQP2 in the HF groups could be due to changes in intrarenal AT1R expression in IM. Immunoblots are presented in Fig. 6 and the corresponding data in Table 7.

Table 4. Inner medullary expression of AQP2 and p-AQP2.

AQP2			
A	Sham	HF	L-Sham
n	7	6	8
Fraction of Sham	100 ± 10	91 ± 3	66 ± 6*#
B	Sham	L-HF	L-Sham
n	7	7	8
Fraction of Sham	100 ± 11	85 ± 6	68 ± 7*
C	HF	L-HF+d	L-HF
n	6	8	7
Fraction of HF	100 ± 5	68 ± 3#†	78 ± 4#
D	L-Sham	L-HF+d	L-Sham+d
n	8	8	8
Fraction of L-Sham	100 ± 9	76 ± 1‡	145 ± 10‡†
E	Sham	L-Sham+d	L-Sham
n	7	8	8
Fraction of Sham	100 ± 10	103 ± 6	69 ± 8*♣
p-AQP2			
F	Sham	HF	L-Sham
n	7	6	8
Fraction of Sham	100 ± 7	108 ± 4	79 ± 5*#
G	Sham	L-HF	L-Sham
n	7	7	8
Fraction of Sham	100 ± 9	91 ± 5	74 ± 6*
H	HF	L-HF+d	L-HF
n	6	8	7
Fraction of HF	100 ± 8	73 ± 6#	81 ± 3#
I	L-Sham	L-HF+d	L-Sham+d
n	8	8	8
Fraction of L-Sham	100 ± 8	84 ± 7	122 ± 5‡†
J	Sham	L-Sham+d	L-Sham
n	7	8	8
Fraction of Sham	100 ± 6	109 ± 4	78 ± 4*♣

Values are expressed as means ± SE. AQP2, aquaporin-2;

p-AQP2, p(Ser256)-aquaporin-2;

n, number of rats.

**P* < 0.05 vs. Sham

P < 0.05 vs. HF

† *P* < 0.05 vs. L-HF+d

‡ *P* < 0.05 vs. L-Sham

♣ *P* < 0.05 vs. L-Sham+d. Values are expressed as means ± SE.

doi:10.1371/journal.pone.0116501.t004

AT1R protein abundances were downregulated in HF and L-HF vs. both Sham and L-Sham (Fig. 6, A and B). Furthermore, AT1R from L-HF+d was decreased vs. HF and L-HF and vs. L-Sham and L-Sham+d (Fig. 6, C and D). No changes were observed between sham groups (Fig. 6, E).

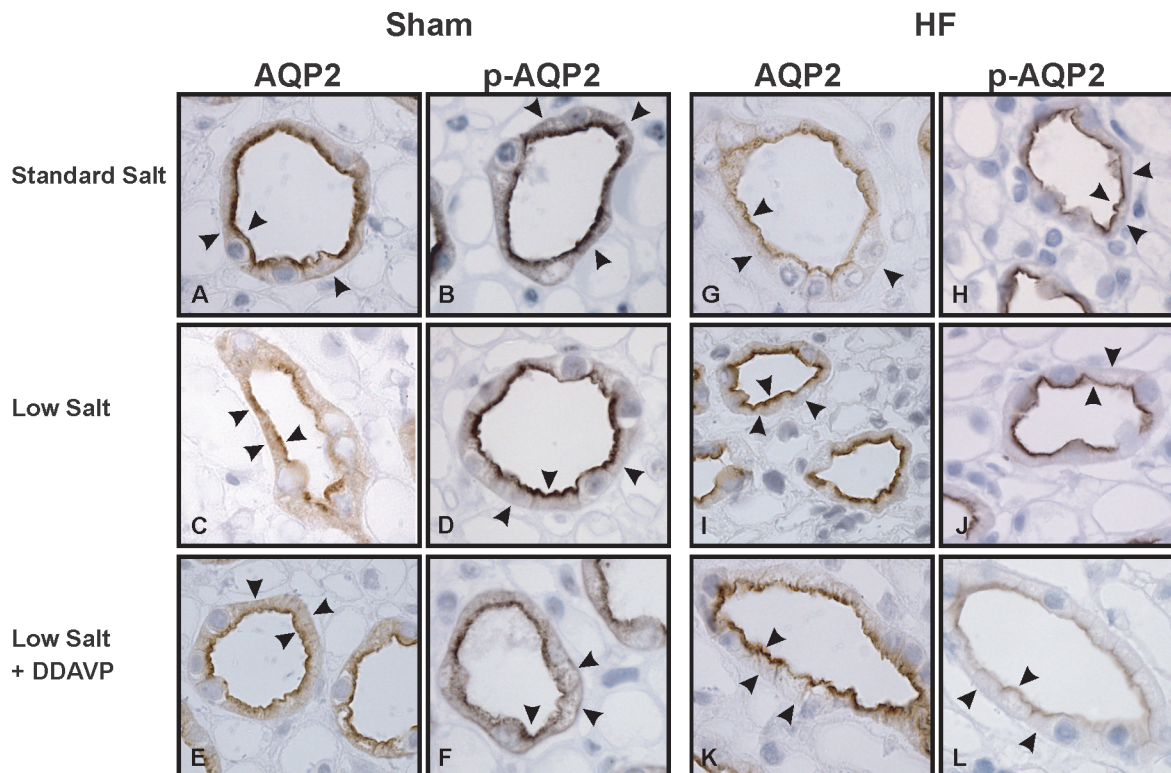


Fig 3. AQP2 and p-AQP2 IMCD localization. Immunoperoxidase microscopy of AQP2 and p-AQP2 in the inner medulla. Sections were incubated with affinity-purified anti-AQP2 (A – E) or affinity-purified anti-p-AQP2 antibody (F – J), and labeling was visualized using peroxidase-conjugated secondary antibody. A – B: In standard salt diet Sham rats AQP2 and p-AQP2 labeling is present at the apical and intracellular domains (arrows). C – F: AQP2 and p-AQP2 stainings from L-Sham and L-Sham+d rats were mainly situated in apical domains with weak intracellular labeling. G – L: In contrast, all HF groups demonstrated strong apical immunoperoxidase labeling of AQP2 and p-AQP2 with virtually no staining in intracellular domains. Magnification x 630.

doi:10.1371/journal.pone.0116501.g003

The (pro)renin receptor is upregulated in L-HF but not in L-Sham rats

The (pro)renin receptor ((P)RR) is expressed in intercalated type A cells in the collecting ducts (CD). In addition, soluble (P)RR is secreted into the tubular lumen. (P)RR has been shown to induce ANG I formation from angiotensinogen (AGT) from the proximal tubules (for review, see [39]). As the late CD's contain angiotensin-converting enzyme facilitating the conversion of ANG I into ANG II which could modulate the regulation of water channels, we wanted to test whether changes in (P)RR abundance could play a role in the pathophysiology of early-stage HF, and whether this could be altered by RAS enhancement or clamped high-level DDAVP. Immunoblots are presented in Fig. 7 and the corresponding data in Table 8. No change in IM (P)RR was observed between Sham rats, L-Sham, and HF (Fig. 7, A). (P)RR was mildly increased in L-HF vs. Sham and the other HF groups but remained unchanged vs. L-Sham (Fig. 7, B and C). In contrast, L-Sham+d and L-HF+d decreased (P)RR levels vs. L-Sham. (Fig. 7, D).

Inner medullary expression of AQP3 and Na-K-ATPase

The abundance of the basolateral water channel AQP3 has previously been shown to remain unchanged in chronic stage HF rats [11]. AQP3 is partly regulated by AVP [40]. Thus, IM AQP3 could be altered in early-stage HF. Data are presented in Table 9. Semiquantitative immunoblotting showed that all groups maintained unchanged AQP3 protein levels, except L-HF

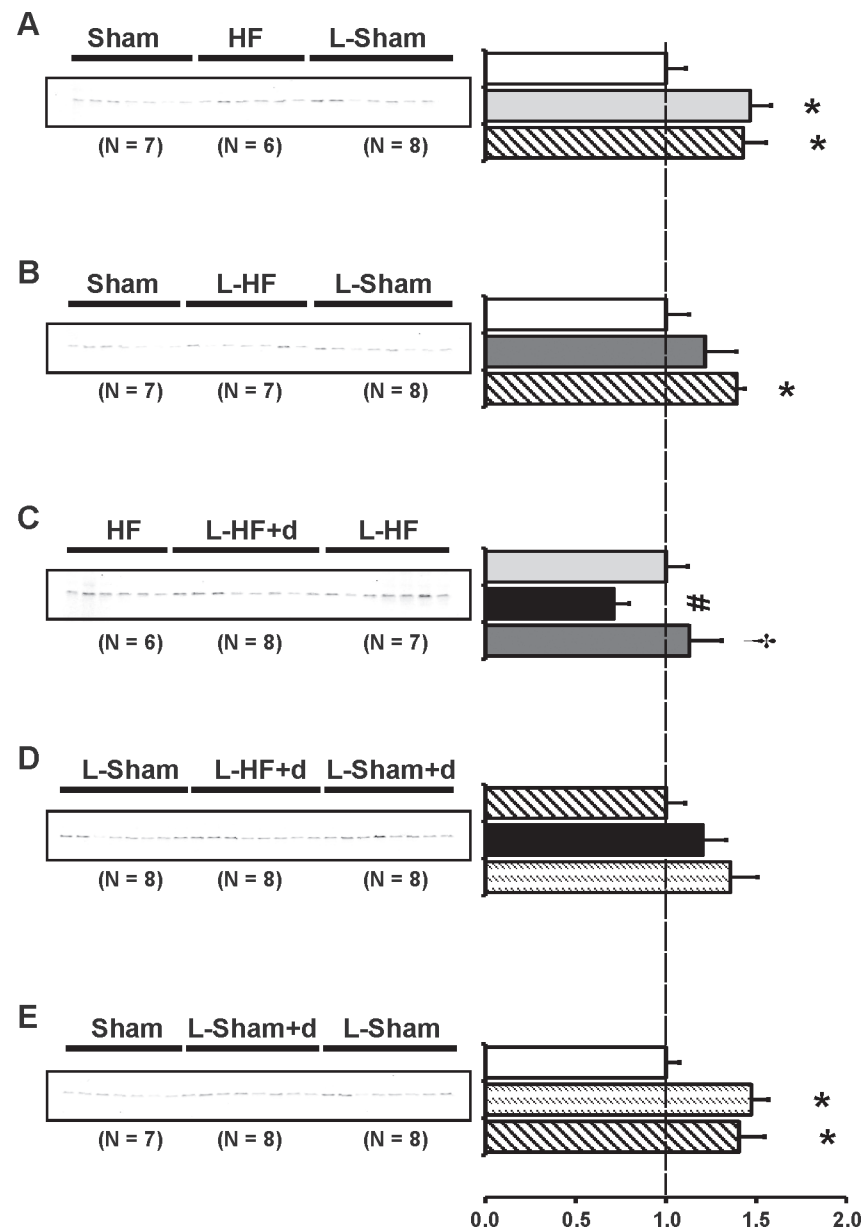


Fig 4. V2 vasopressin receptor abundance. Semiquantitative immunoblotting of kidney protein prepared from inner medulla. Immunoblot was reacted against anti-V2R protein and revealed a single band at ~ 47 kDa (A-E). Data are presented in Table 5. A) Densitometry revealed increased V2R expression in HF vs. Sham. A significant V2R increase was also present in L-Sham vs. Sham, as also seen in (B) and (E). B) The V2R expression between Sham and L-HF was comparable. C) Decreased V2R protein expression in L-HF+d vs. HF and L-HF was observed, whereas standard diet HF and L-HF was comparable. D) No statistical differences were found among groups. E) V2R abundance was increased in L-Sham+d and L-Sham vs. Sham, whereas L-Sham+d and L-Sham remained unchanged. Each column represents the mean \pm SE. Solid white, Sham; solid light grey, HF; line pattern, L-Sham; solid dark grey, L-HF; solid black, L-HF+d; dotted pattern, L-Sham+d. * $P < 0.05$ vs. Sham, # $P < 0.05$ vs. HF, † $P < 0.05$ vs. L-HF+d.

doi:10.1371/journal.pone.0116501.g004

+d which downregulated AQP3 expression compared with HF (Table 9, C) and L-Sham (Table 9, D), respectively. In addition, we investigated whether Na-K-ATPase protein expression was altered, as seen in previous studies [41], however no changes were observed (Table 9, A – E).

Table 5. Inner medullary expression of the V2 vasopressin receptor.

V2R			
A	Sham	HF	L-Sham
n	7	6	8
Fraction of Sham	100 ± 11	147 ± 12*	143 ± 13*
B	Sham	L-HF	L-Sham
n	7	7	8
Fraction of Sham	100 ± 13	122 ± 17	139 ± 5*
C	HF	L-HF+d	L-HF
n	6	8	7
Fraction of HF	100 ± 12	71 ± 8#	113 ± 18†
D	L-Sham	L-HF+d	L-Sham+d
n	8	8	8
Fraction of L-Sham	100 ± 11	120 ± 13	144 ± 15
E	Sham	L-Sham+d	L-Sham
n	7	8	8
Fraction of Sham	100 ± 7	147 ± 10*	140 ± 14*

Values are expressed as means ± SE. V2R, V2 vasopressin receptor;

n, number of rats.

**P* < 0.05 vs. Sham

P < 0.05 vs. HF

† *P* < 0.05 vs. L-HF+d.

doi:10.1371/journal.pone.0116501.t005

Inner medullary AQP1 abundance is decreased in low sodium diet Sham rats

AQP1 is constitutively expressed in IM thin descending limbs origin from long loop nephrons [42]. AQP1 is critical for urine concentration ability. Thus, we wanted to test AQP1 protein abundance in response to low sodium diet and DDAVP in early-stage HF, as these factors could alter IM tonicity [43]. Immunoblots are presented in Fig. 8 and the corresponding data in Table 10. AQP1 abundance remained unaffected in all the HF-groups, also when compared to Sham (Fig. 8, A, B, and C). In contrast, AQP1 was downregulated in L-Sham and L-Sham+d vs. Sham (Fig. 8, E).

Inner medullary AQP4 is increased in HF and L-HF rats

AQP4 is present at the basolateral membrane on IM principal cells where it in conjunction with AQP3 is facilitating water transport to the intracellular space [44]. Thus, we tested whether AQP4 could play a role in the fine tuning of IM free water reabsorption in HF and in settings where ANG II and V2R stimulation is increased. Immunoblots are presented in Fig. 9 and the corresponding data in Table 11. AQP4 abundance increased in HF, and L-HF, L-sham, and L-Sham+d vs. Sham (Fig. 9, A, B, and E). In contrast, L-HF+d downregulated AQP4 vs. HF, L-HF, L-Sham, and L-Sham+d (Fig. 9, C and D).

Discussion

HF rats developed hyponatremia, hypo-osmolality, increased HR, and decreased levels of fractional urinary excretion of sodium, but exhibited comparable IM AQP2 and p-AQP2 abundance with Sham rats 17 days after MI. In previous HF studies 21, 29 and 34 days after MI,

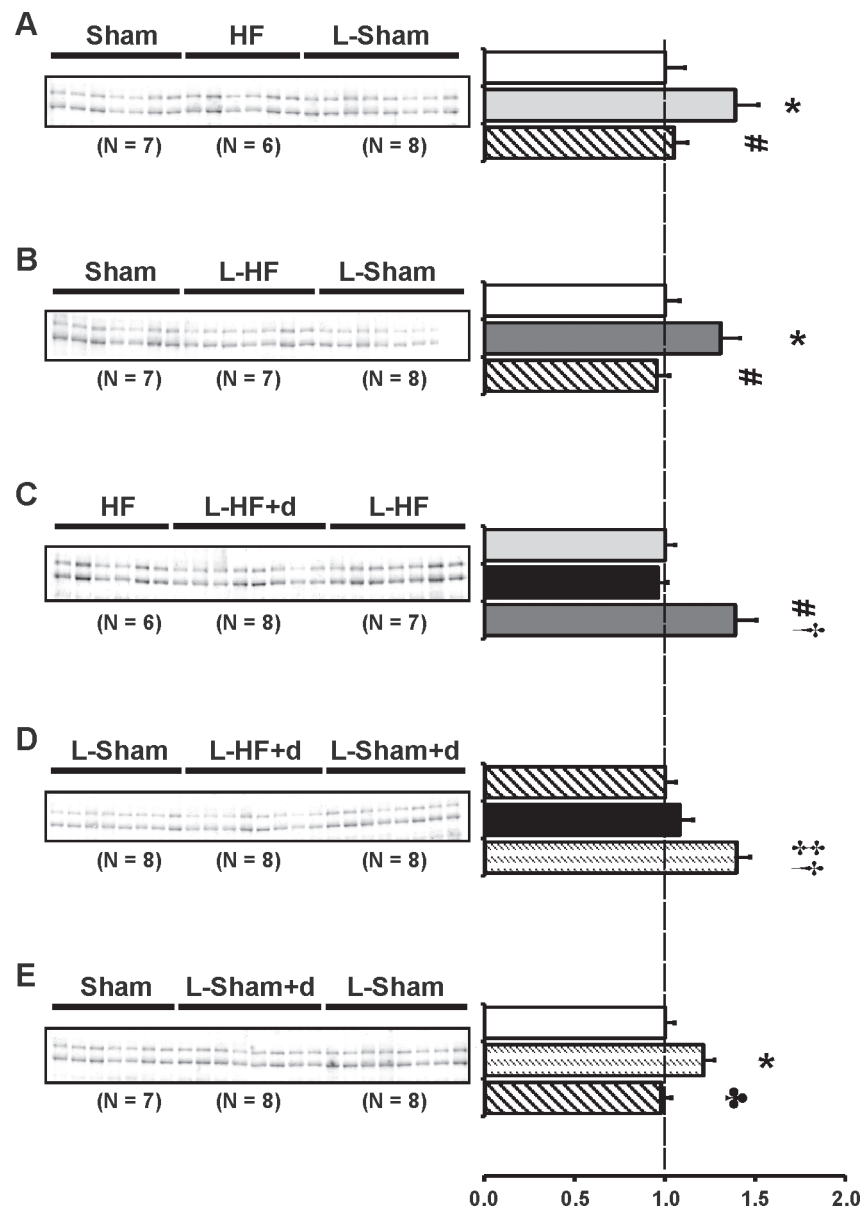


Fig 5. Gsα subunit abundance. Semiquantitative immunoblotting of kidney protein prepared from inner medulla. Immunoblot was reacted against anti-Gsα subunit of the G-protein revealing a doublet band at 45 and 50 kDa (A-E). Data are presented in Table 6. A) Densitometric analysis revealed significantly increased Gsα abundance in HF vs. Sham and L-Sham, whereas Gsα expression was comparable between Sham and L-Sham, as also presented in (B) and (E). B) Gsα was increased in L-HF vs. Sham and L-Sham. C) Gsα abundance was increased in L-HF rats vs. HF and L-HF+d, whereas Gsα expressions were comparable between HF and L-HF+d. D) Gsα abundance was increased in L-Sham+d rats vs. L-Sham rats and L-HF+d. L-Sham and L-HF+d groups were comparable. E) As observed in (D), Gsα abundances in L-Sham+d rats were increased vs. Sham and L-Sham. Each column represents the mean ± SE. Solid white, Sham; solid light grey, HF; line pattern, L-Sham; solid dark grey, L-HF; solid black, L-HF+d; dotted pattern, L-Sham+d. * $P < 0.05$ vs. Sham, # $P < 0.05$ vs. HF, † $P < 0.05$ vs. L-HF+d, ‡ $P < 0.05$ vs. L-Sham, ♣ $P < 0.05$ vs. L-Sham+d.

doi:10.1371/journal.pone.0116501.g005

upregulation of AQP2 and distribution of AQP2 and p-AQP2 to apical domains in IMCD was observed [2,9,11,45]. Here we demonstrate that in early-stage HF, IMCD AQP2 and p-AQP2 are located in apical domains whereas AQP2 protein abundance remains comparable with

Table 6. Inner medullary expression of the Gsa subunit.

Gsa			
A	Sham	HF	L-Sham
n	7	6	8
Fraction of Sham	100 ± 11	139 ± 13*	105 ± 8#
B	Sham	L-HF	L-Sham
n	7	7	8
Fraction of Sham	100 ± 8	131 ± 11*	95 ± 7#
C	HF	L-HF+d	L-HF
n	6	8	7
Fraction of HF	100 ± 6	96 ± 5	139 ± 12#†
D	L-Sham	L-HF+d	L-Sham+d
n	8	8	8
Fraction of L-Sham	100 ± 6	108 ± 8	140 ± 7†‡
E	Sham	L-Sham+d	L-Sham
n	7	8	8
Fraction of Sham	100 ± 5	121 ± 6*	98 ± 6♣

Values are expressed as means ± SE. Gsa, Gsa subunit; n, number of rats.

* $P < 0.05$ vs. Sham

$P < 0.05$ vs. HF

† $P < 0.05$ vs. L-HF+d

‡ $P < 0.05$ vs. L-Sham

♣ $P < 0.05$ vs. L-Sham+d.

doi:10.1371/journal.pone.0116501.t006

Sham rats. This strongly indicates for the first time that the transit to chronically elevated AQP2 levels in HF happens in coordination with the finalization of myocardial remodeling.

HF groups and sodium restricted sham rats had comparable decrements in plasma sodium and osmolality

All HF groups were hyponatremic with decreased plasma osmolality, disregarded the type of diet. HF rats on standard diet developed milder hyponatremia than the other groups. We used dietary sodium depletion and DDAVP administration to further enhance the effect of circulating ANG II and AVP. In previous studies using the same HF model, the HF rats had increased plasma levels of renin, ANG II, aldosterone, and AVP, in addition to increased abundance and apical targeting of AQP2, even when normonatremic and disregarding changes in plasma osmolality [2,9,46]. Hence, our present findings suggest that even in early-stage HF, elevated ANG II and AVP can mediate avid water retention. Sodium restricted sham groups lowered plasma sodium and osmolality to levels comparable with the HF groups. It is however surprising, that the L-HF+d and L-Sham+d rats displayed increased plasma osmolality compared with L-HF, despite of reduced urine output and comparable water intake, because plasma urea was also unchanged. We cannot fully explain this finding. However, on the last day of experiment, urine output in the L-HF+d rats was as low as $8.2 \pm 1.2 \mu\text{l} \cdot \text{min}^{-1} \cdot \text{kg}^{-1}$, almost half the output of the L-HF group. Therefore, a degree of uremia which in part can account for the increased plasma osmolality in the L-HF+d rats group cannot be ruled out. Nevertheless, the HF groups in our study managed to maintain AQP2 and p-AQP2 abundance within sham levels

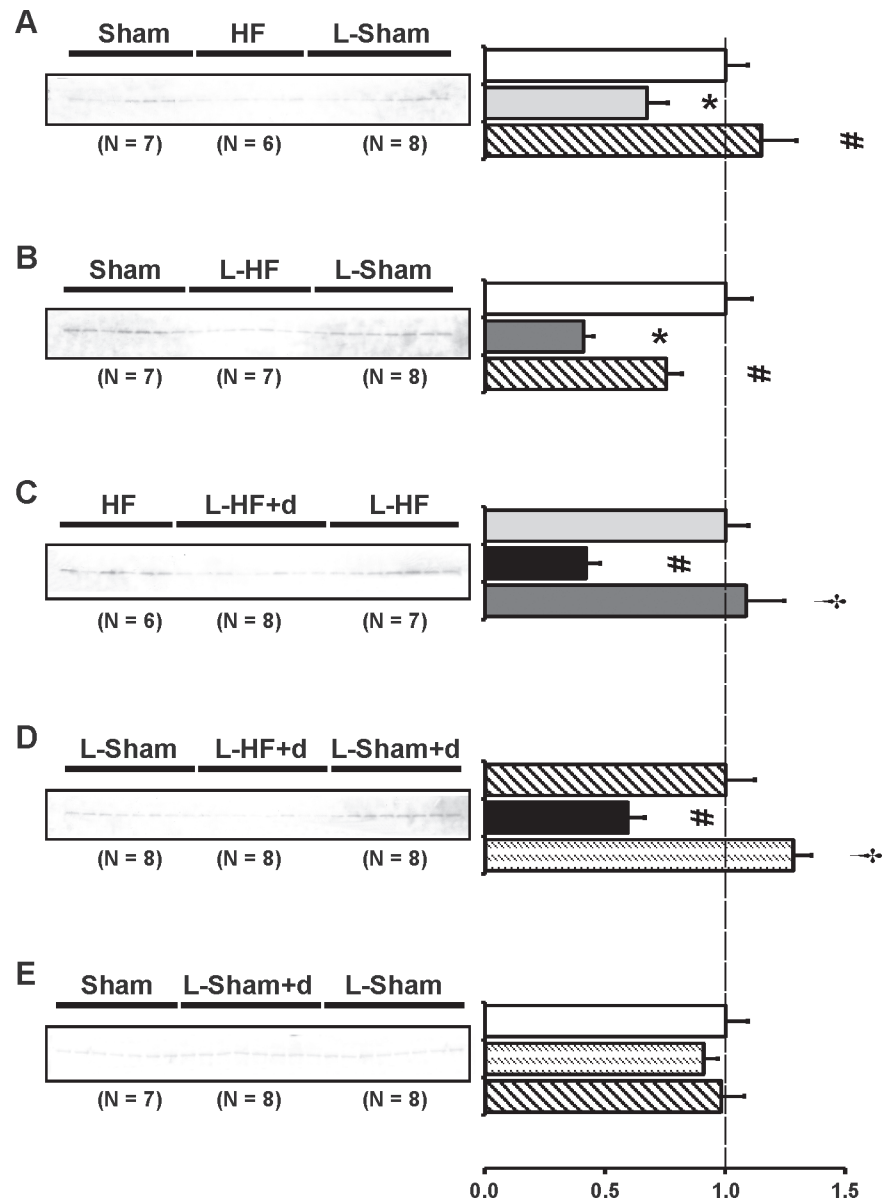


Fig 6. Type 1_A angiotensin II receptor abundance. Semiquantitative immunoblotting of kidney protein prepared from inner medulla. Immunoblot was reacted with anti-AT1R revealing a single band at ~ 43 kDa (A-E). Data are presented in Table 7. (A and B) Analysis revealed significantly decreased AT1R expression in HF and L-HF vs. Sham and vs. L-Sham, respectively. AT1R expression was comparable in Sham and L-Sham. C) When compared with HF and L-HF, AT1R protein expression was decreased in the L-HF+d rats, whereas levels between HF and L-HF were comparable. D) Decreased expression of AT1R was observed in L-HF+d rats when compared with L-Sham and L-Sham+d, whereas AT1R levels between L-Sham and L-Sham+d were comparable, as also presented in E). E) AT1R protein expression was comparable between Sham, L-Sham and L-Sham+d. Each column represents the mean ± SE. Solid white, Sham; solid light grey, HF; line pattern, L-Sham; solid dark grey, L-HF; solid black, L-HF+d; dotted pattern, L-Sham+d. * $P < 0.05$ vs. Sham, # $P < 0.05$ vs. HF, † $P < 0.05$ vs. L-HF+d.

doi:10.1371/journal.pone.0116501.g006

under physiological and hormonal conditions well-known to otherwise promote AQP2 abundance, suggesting activation of a compensating mechanism in early-stage HF not previously described [47,48].

Table 7. Inner medullary expression of the type 1_A angiotensin II receptor.

AT1R			
A	Sham	HF	L-Sham
n	7	6	8
Fraction of Sham	100 ± 9	67 ± 9*	115 ± 15#
B	Sham	L-HF	L-Sham
n	7	7	8
Fraction of Sham	100 ± 11	41 ± 4*	75 ± 6#
C	HF	L-HF+d	L-HF
n	6	8	7
Fraction of HF	100 ± 10	42 ± 6#	109 ± 16†
D	L-Sham	L-HF+d	L-Sham+d
n	8	8	8
Fraction of L-Sham	100 ± 12	59 ± 7#	128 ± 8†
E	Sham	L-Sham+d	L-Sham
n	7	8	8
Fraction of Sham	100 ± 9	91 ± 6	98 ± 10

Values are expressed as means ± SE. AT1R, type 1_A angiotensin II receptor;
n, number of rats.

**P* < 0.05 vs. Sham

P < 0.05 vs. HF

† *P* < 0.05 vs. L-HF+d.

doi:10.1371/journal.pone.0116501.t007

Vasopressin-induced AQP2 and p-AQP2 upregulation was blunted in early-stage HF after MI

Previous studies have shown that sodium restricted rats subjected to long-term DDAVP administration increased IM AQP2 and p-AQP2 [8]. We observed the same response in the L-Sham+d rats in our study. In the study by Kwon et al., AQP2 and p-AQP2 abundance was restored to control levels by co-treatment with the specific AT1R blocker candesartan [8]. Likewise, chronic-stage HF rats with elevated plasma ANG II levels reversed the observed increased protein expression and apical targeting of AQP2 and p-AQP2 in the IMCD after candesartan treatment [9]. In the present study, HF groups decreased AT1R protein abundance but elevated V2R and Gsα protein, indicating activation of the 3'-5'-cyclic adenosine monophosphate (cAMP)/protein kinase A (PKA) pathway [10]. AT1R is situated throughout the entire nephron including renal interstitial cells and vasculature to allow regulation of glomerular filtration rate (GFR), renal blood flow, and water and salt reabsorption [49]. Thus, there are strong indications that crosstalk between the AVP and ANG II signaling pathways is possible and important in HF. However, the underlying mechanism in V2R-AT1R crosstalk is still debated.

AVP-binding to V2R increases cAMP levels and mobilizes intracellular [Ca²⁺] stores in IMCD which in turn promotes AQP2-trafficking to the apical plasma membrane [50–53]. It has been suggested that Ca²⁺ is necessary for the insertion of AQP2 into the apical plasma membrane through calmodulin-dependent release from ryanodine-sensitive intracellular Ca²⁺ stores [54,55]. Furthermore, AQP2 trafficking can also be modulated through V2R regulated Ca²⁺ flux without affecting [cAMP] and through activation of the cAMP sensor protein Epac (exchange protein directly activated by cAMP) [10,56,57].

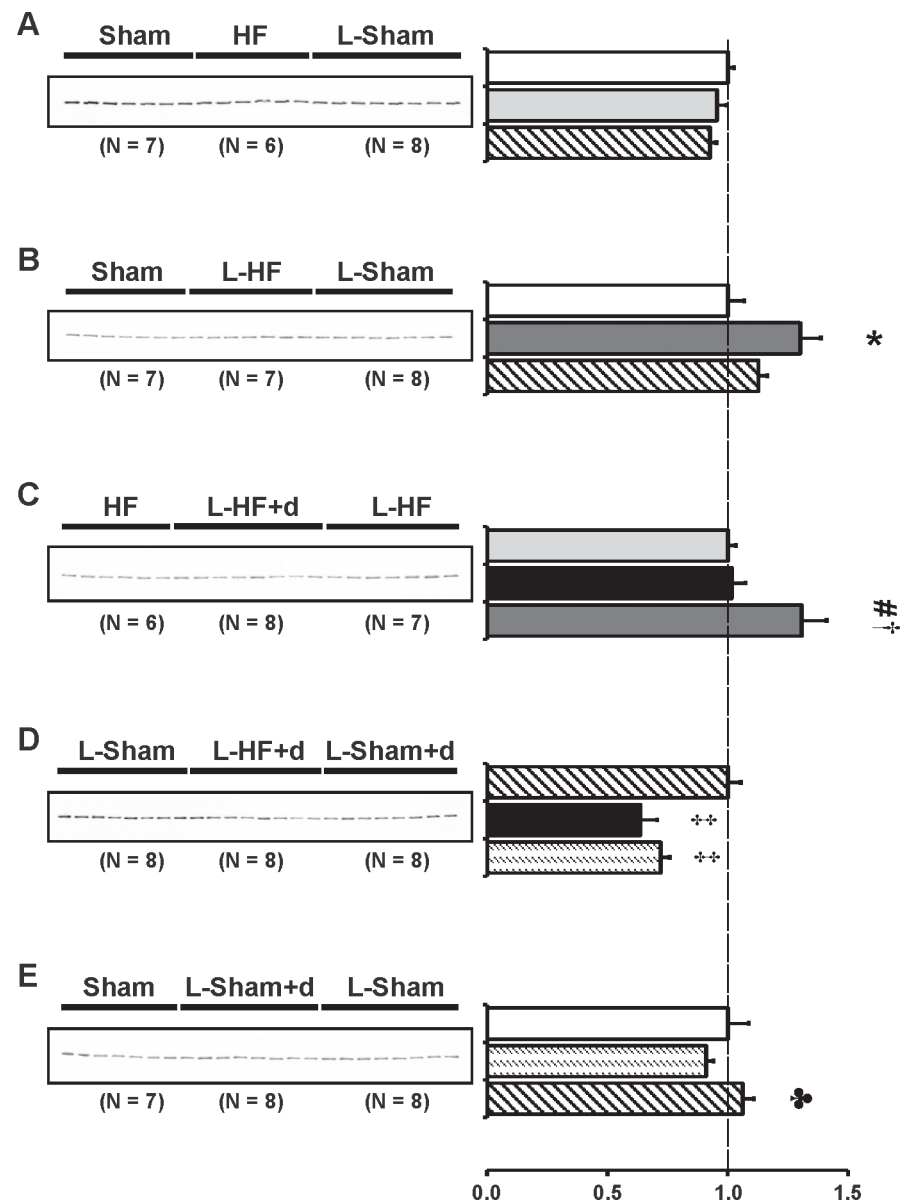


Fig 7. (Pro)renin receptor abundance. Semiquantitative immunoblotting of kidney protein prepared from inner medulla. Immunoblot was reacted with a specific antibody against anti-(P)RR revealing a single band at ~ 42 kDa (A-E). Data are presented in Table 8. (A and B) (P)RR expression was increased in L-HF vs. Sham and L-Sham, whereas no difference in (P)RR protein expression between Sham, HF or L-Sham was found. As also presented in A) and E), no difference was observed between Sham and L-Sham rats. C) (P)RR expression increased in L-HF vs. HF and L-HF+d, whereas no difference was observed between HF and L-HF+d. D) Densitometry revealed significantly decreased (P)RR abundance in L-HF+d and L-Sham+d when compared with L-Sham. The decrease in L-HF+d and L-Sham+d was comparable. E) As already shown, densitometry revealed that L-Sham+d decreased (P)RR expression compared with L-Sham, and no difference was found between Sham and L-Sham. Each column represents the mean \pm SE. Solid white, Sham; solid light grey, HF; line pattern, L-Sham; solid dark grey, L-HF; solid black, L-HF+d; dotted pattern, L-Sham+d. * $P < 0.05$ vs. Sham, # $P < 0.05$ vs. HF, † $P < 0.05$ vs. L-HF+d, ‡ $P < 0.05$ vs. L-Sham, ♣ $P < 0.05$ vs. L-Sham+d.

doi:10.1371/journal.pone.0116501.g007

Table 8. Inner medullary expression of the (pro)renin receptor.

(P)RR			
A	Sham	HF	L-Sham
n	7	6	8
Fraction of Sham	100 ± 2	95 ± 4	92 ± 3
B	Sham	L-HF	L-Sham
n	7	7	8
Fraction of Sham	100 ± 7	130 ± 9*	113 ± 4
C	HF	L-HF+d	L-HF
n	6	8	7
Fraction of HF	100 ± 3	102 ± 6	131 ± 10#†
D	L-Sham	L-HF+d	L-Sham+d
n	8	8	8
Fraction of L-Sham	100 ± 5	64 ± 7‡	72 ± 4‡
E	Sham	L-Sham+d	L-Sham
n	7	8	8
Fraction of Sham	100 ± 9	92 ± 3	106 ± 5♣

Values are expressed as means ± SE. (P)RR, (pro)renin receptor; n, number of rats.

* $P < 0.05$ vs. Sham

$P < 0.05$ vs. HF

† $P < 0.05$ vs. L-HF+d

‡ $P < 0.05$ vs. L-Sham

♣ $P < 0.05$ vs. L-Sham+d.

doi:10.1371/journal.pone.0116501.t008

In general, ANG II induces a rise in intracellular $[Ca^{2+}]$ by inositol 1,4,5-triphosphate [58] and PKC activation by PLC mediated formation of the second messenger diacylglycerol (DAG) [59]. ANG II also has the capability to induce a large variety of additional intracellular signal cascades involving AQP2 regulation, including phosphorylated mitogen-activated protein (MAP) kinase, extracellular signal-regulated kinase 1/2 (ERK1/2), p38 kinase, and phosphatidylinositol 3'-kinase [60]. Evidence of PKC mediated cAMP accumulation has been shown in transfected HEK-293 cells. More direct potentiation of cAMP accumulation by ANG II through activation of protein kinase C (PKC) and intracellular Ca^{2+} release has also been shown. Here, ANG II enhanced DDAVP-mediated AQP2 targeting in V2R and AT1R transfected Chinese hamster ovary cells and in primary cultured IMCD cells [10,55]. Since rise in intracellular $[Ca^{2+}]$ induced by thapsigargin did not enhance cAMP accumulation when adding AVP, it was concluded that Ca^{2+} flux is less likely to be the prime mechanism of AT1R-V2R crosstalk [10]. However, some inconsistency exists in the current literature. For example, thapsigargin increased intracellular $[Ca^{2+}]$ in rat cardiac fibroblasts and potentiated isoproterenol- and forskolin-stimulated cAMP production. This study suggests that ANG II mediated potentiation of cAMP is facilitated by phospholipase C (PLC) through G_q activation and internal Ca^{2+} release rather than the major PKC pathway [61]. In consistency, cAMP-independent activation of AQP2 involving intracellular Ca^{2+} release was shown in rat IMCD in a manner suggesting V2R action of phosphoinositide-specific PLC [52]. Also in favor of the PLC hypothesis, PKC has in several other studies been shown to enhance AQP2 endocytosis instead of apical trafficking. The underlying mechanism has been suggested to be mediated by actin cytoskeletal

Table 9. Inner medullary expression of AQP3 and Na-K-ATPase.

A	Sham	HF	L-Sham
n	7	6	8
AQP3	100 ± 14	107 ± 18	99 ± 9
Na-K-ATPase	100 ± 31	67 ± 23	100 ± 20
B	Sham	L-HF	L-Sham
n	7	7	8
AQP3	100 ± 14	103 ± 16	93 ± 10
Na-K-ATPase	100 ± 26	87 ± 18	73 ± 17
C	HF	L-HF+d	L-HF
n	6	8	7
AQP3	100 ± 15	57 ± 11#	69 ± 11
Na-K-ATPase	100 ± 37	134 ± 27	121 ± 23
D	L-Sham	L-HF+d	L-Sham+d
n	8	8	8
AQP3	100 ± 8	59 ± 11‡	82 ± 10
Na-K-ATPase	100 ± 25	120 ± 26	98 ± 23
E	Sham	L-Sham+d	L-Sham
n	7	8	8
AQP3	100 ± 12	108 ± 10	93 ± 9
Na-K-ATPase	100 ± 29	103 ± 26	112 ± 25

Values are expressed as means ± SE. AQP3, aquaporin-3;

Na-K-ATPase, Na-K-ATPase;

n, number of rats.

$P < 0.05$ vs. HF

‡ $P < 0.05$ vs. L-Sham.

doi:10.1371/journal.pone.0116501.t009

rearrangements and transient short-chain ubiquitination of AQP2 after either AVP withdrawal or activation of PKC independently of p(S256)-AQP2 abundance [62–65]. Thus, further investigations are needed to fully reveal the downstream mechanisms in AT1R-V2R crosstalk.

Apical expressions of AQP2 and p-AQP2 in HF groups were increased

Additional immunohistochemistry revealed that all HF groups in our study developed marked apical labeling of AQP2 and p-AQP2 in IMCD compared to standard diet sham rats, despite decreased AT1R. Our study is consistent with previous results in mice lacking AT1_A receptors only in the collecting duct (CD-KO). When water deprived, these mice diminished AQP2 abundance but sustained almost complete apical targeting of IMCD AQP2 in response to AVP stimulation [49]. One possible explanation could be that ANG II-AT1R complexes situated in earlier nephron segments could modulate flow rate and tonicity of the tubular fluid entering the medullary collecting ducts, and thereby influence AQP2 trafficking. For example, hypotonicity favors internalization of p-AQP2 and AQP2 in cultured renal CD8 cells, whereas hypertonicity enhances apical and basolateral AQP2 membrane accumulation in the IMCD [38,66–68]. Consistently, we have previously demonstrated that complete and global AT1R inhibition with candesartan reversed apical targeting of IMCD AQP2 and p-AQP2 in chronic HF rats [9]. Moreover, enhanced apical labeling of AQP2 and p-AQP2 in IMCD could also simply reflect increased AVP activity. Evidence of enhanced accumulation of cAMP in HF suggesting increased V2R activity has

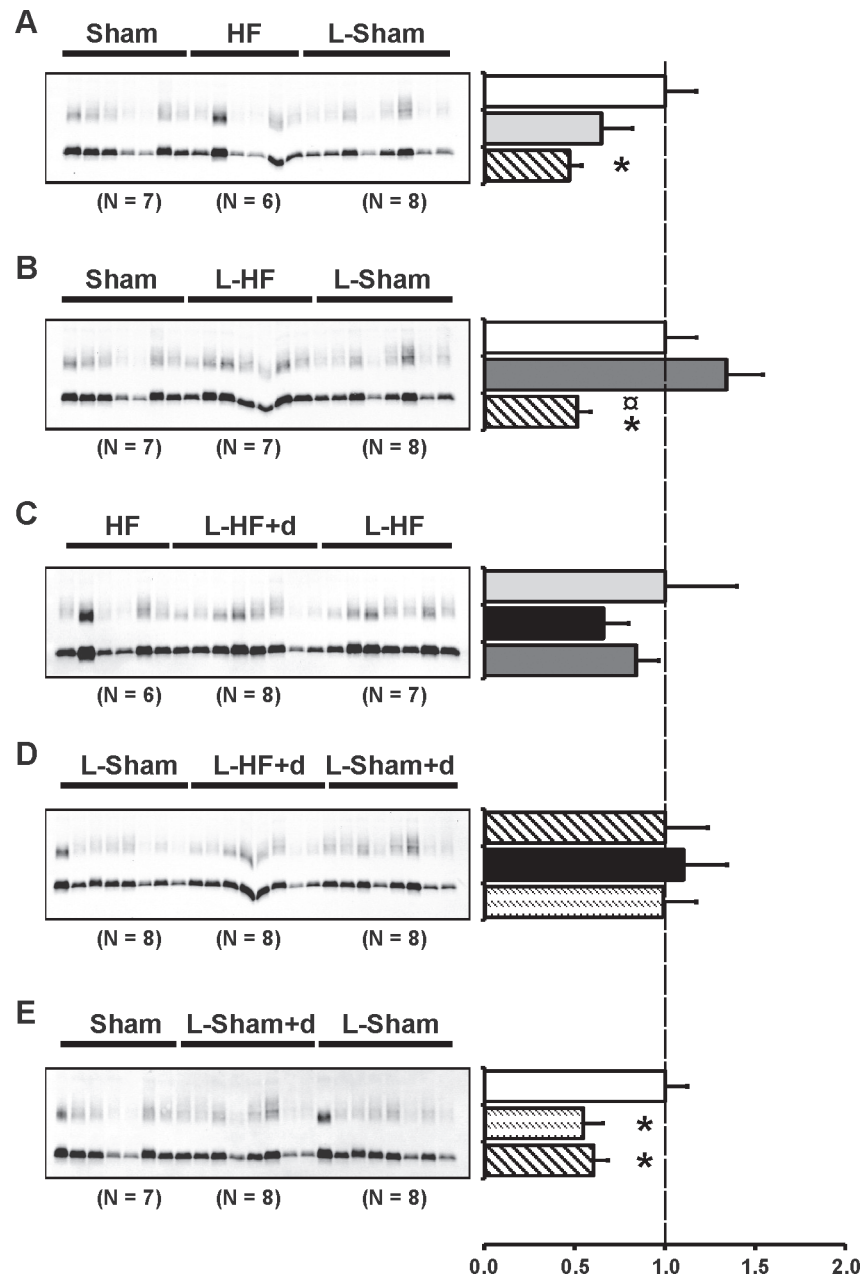


Fig 8. AQP1 abundance. Semiquantitative immunoblotting of kidney protein prepared from inner medulla. Immunoblot was reacted with anti-AQP1 antibody and reveals 29 kDa and 35–50 kDa AQP1-bands (A–E). Data are presented in Table 9. A) L-Sham was decreased vs. Sham and HF, as also presented in (B) and (E). No difference was found between Sham and HF. B) No difference was observed between Sham and L-HF. C) HF, L-HF+d, and L-HF had comparable AQP1 protein levels. D) Densitometric analysis revealed that L-Sham, L-HF+d, and L-Sham+d had comparable AQP1 protein levels. Each column represents the mean \pm SE. Solid white, Sham; solid light grey, HF; line pattern, L-Sham; solid dark grey, L-HF; solid black, L-HF+d; dotted pattern, L-Sham+d. * $P < 0.05$ vs. Sham, \square * $P < 0.05$ vs. L-HF.

doi:10.1371/journal.pone.0116501.g008

already been shown in Isolated IMCDs from HF rats and cardiomyopathic hamsters [46,69]. Recently, Brønd et al demonstrated that V2R-mediated cAMP accumulation was associated with elevated IM AQP2 protein expression and a fast recycling within 30 minutes of surface-associated V2R in HF rats, whereas the V2R in isolated IMCDs from control rats did not recycle to the

Table 10. Inner medullary expression of AQP1.

AQP1			
A	Sham	HF	L-Sham
n	7	6	8
Fraction of Sham	100 ± 17	65 ± 17	47 ± 7*
B	Sham	L-HF	L-Sham
n	7	7	8
Fraction of Sham	100 ± 17	134 ± 20	51 ± 7*α
C	HF	L-HF+d	L-HF
n	6	8	7
Fraction of HF	100 ± 40	66 ± 14	84 ± 13
D	L-Sham	L-HF+d	L-Sham+d
n	8	8	8
Fraction of L-Sham	100 ± 24	110 ± 24	99 ± 18
E	Sham	L-Sham+d	L-Sham
n	7	8	8
Fraction of Sham	100 ± 12	55 ± 11*	60 ± 8*

Values are expressed as means ± SE. AQP1, aquaporin-1;

n, number of rats. L-Sham+d.

* $P < 0.05$ vs. Sham

α $P < 0.05$ vs. L-HF.

doi:10.1371/journal.pone.0116501.t010

receptor surface after AVP stimulation [46]. In another study by the same group using isolated medullary thick ascending limbs from HF rats, the enhanced AVP-V2R sensibility shown by cAMP accumulation was completely blocked by the AT1R blocker losartan [70]. Furthermore, administration of an angiotensin-converting enzyme inhibitor to HF rats normalized the increased AQP2 mRNA levels and restored GFR to sham levels [7,71]. These results are in line with our study, suggesting that ANG II is able to exert direct modulations on the V2R-mediated PKA pathway, resulting in enhanced apical targeting of total AQP2.

In the present study, HF rats spontaneously decreased receptor AT1R abundance at least in the IMCD, presumably as a result of high levels of circulating ANG II and enhanced AT1R activation. Even so, the rats preserved high levels of apical shuttling. Consistently, mice lacking the AT1R only in the collecting duct (CD-KO mice) showed substantial apical targeting when stimulated with DDAVP vs. controls. Interestingly, the CD-KO mice only reduced AT1_A mRNA levels by 43 ± 6.5% vs. controls in IMCD, indicating a residual amount of AT1R [8,9,49]. The observed differences in AQP2 targeting among the present and previous studies using AT1R blockage may be due to the quantity of still active AT1R in the IMCD in the CD-KO mice with a rather low threshold for potentiating AQP2 targeting [49]. Furthermore, the L-Sham+d rats displayed higher Gsα abundance than the L-HF+d rats, which could reflect differences in V2R activity. However, HF and L-HF rats also increased Gsα abundance vs. Sham and L-Sham (Fig. 5, A and B) similar to L-Sham+d (Fig. 5, E) but still failed to increase AQP2 levels. Based on these observations, we suggest that the effects of AT1R on total AQP2 levels in early-stage HF could be mediated by separate pathways independently of the V2R pathway, despite increased levels of V2R abundance. However, our study does not explain why the compensational effect on AQP2 is only effective when it comes to abundance and not shuttling in early-stage HF, which calls for further investigations.

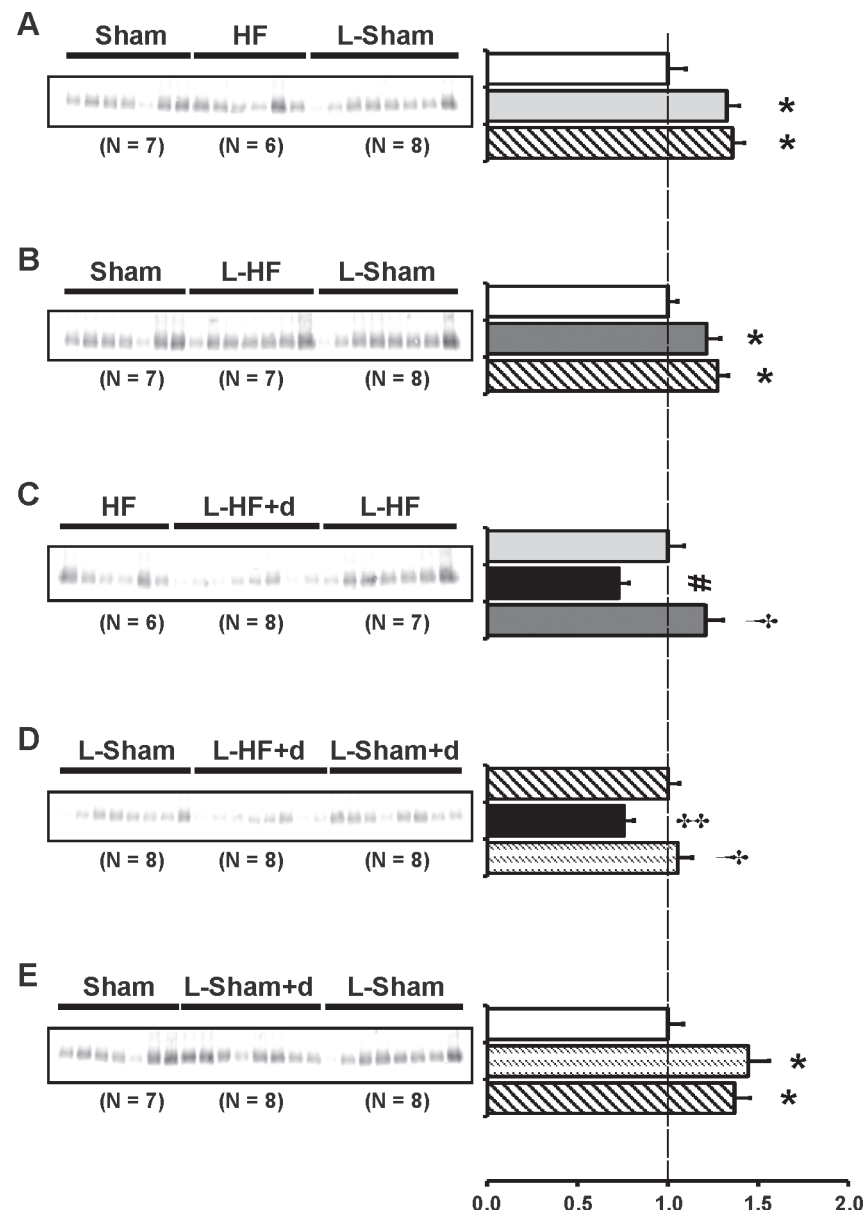


Fig 9. AQP4 abundance. Semiquantitative immunoblotting of kidney protein prepared from inner medulla. Immunoblot was reacted with anti-AQP4 antibody and reveals a single ~ 34.5 kDa AQP4-band (A-E). Data are presented in Table 10. (A-B) Densitometric analysis revealed significantly increased AQP4 protein levels of HF, L-HF and L-Sham vs. Sham. The increase in HF, L-HF and L-Sham was comparable. In contrast, AQP4 protein levels in L-HF+d decreased vs. HF and L-HF in C) and vs. L-Sham and L-Sham+d in D). No difference was observed between L-Sham and L-Sham+d, as also presented in E). E) AQP4 protein levels in L-Sham+d and L-Sham were increased compared with Sham. No difference was observed between L-Sham and L-Sham+d. Each column represents the mean \pm SE. Solid white, Sham; solid light grey, HF; line pattern, L-Sham; solid dark grey, L-HF; solid black, L-HF+d; dotted pattern, L-Sham+d. * $P < 0.05$ vs. Sham, # $P < 0.05$ vs. HF, † $P < 0.05$ vs. L-HF+d, ‡ $P < 0.05$ vs. L-Sham.

doi:10.1371/journal.pone.0116501.g009

The (pro)-renin receptor was increased in L-HF

Apart from ANG I formation, (P)RR has been shown to induce intracellular signaling cascades involving the MAP kinases ERK1/2, which also have been suggested as a modulator of the

Table 11. Inner medullary expression of AQP4.

AQP4			
A	Sham	HF	L-Sham
n	7	6	8
Fraction of Sham	100 ± 10	133 ± 7*	136 ± 7*
B	Sham	L-HF	L-Sham
n	7	7	8
Fraction of Sham	100 ± 5	121 ± 8*	128 ± 6*
C	HF	L-HF+d	L-HF
n	6	8	7
Fraction of HF	100 ± 9	73 ± 6#	121 ± 10†
D	L-Sham	L-HF+d	L-Sham+d
n	8	8	8
Fraction of L-Sham	100 ± 6	76 ± 5‡	105 ± 8†
E	Sham	L-Sham+d	L-Sham
n	7	8	8
Fraction of Sham	100 ± 9	144 ± 12*	137 ± 9*

Values are expressed as means ± SE. AQP4, aquaporin-4;

n, number of rats.

* $P < 0.05$ vs. Sham

$P < 0.05$ vs. HF

† $P < 0.05$ vs. L-HF+d

‡ $P < 0.05$ vs. L-Sham.

doi:10.1371/journal.pone.0116501.t011

V2R-cAMP dependent pathway in AQP2 regulation [72,73]. Shao and coworkers showed that long-term low sodium diet (13 days) increased plasma and intrarenal ANG II, renin and medullary renin mRNA, but failed to increase urinary excretion of angiotensinogen (AGT) and ANG II vs. standard diet rats [18]. Consistently, our study demonstrated that standard diet Sham rats and L-Sham rats had comparable levels of IM AT1R and (P)RR. In contrast, (P)RR was increased in L-HF but decreased in L-HF+d in the presence of lowered AT1R (Fig. 7, D). These data suggest that IM (P)RR is able to be regulated independently of AT1R but might be sensitive to circulating AVP levels, inner medullary osmolality, or both. Decreased AT1R and unaffected V2R levels despite of elevated (P)RR abundance in L-HF could also be part of an escape-mechanism which could be blunted in chronic HF under certain settings where the effect ANG II exceed the effect of AVP. Interestingly, AVP and oxytocin are shown to co-localize with (P)RR in the supraoptic and paraventricular nuclei in human and mouse hypothalamus [74,75]. Furthermore, a recent study using in situ hybridization for (P)RR mRNA and immunohistochemistry double-staining for the pituitary hormones showed that (P)RR mRNA was expressed in most of the GH cells and ACTH cells in the anterior lobe of the pituitary gland, strongly suggesting a central crosstalk between AVP release and (P)RR, but further investigation on this issue is demanded [76].

AQP4 expression is increased in HF and L-HF rats but decreased in L-HF+d

The role IM AQP4 plays in the fine tuning of free water reabsorption is unclear. Whereas targeted disruption of AQP4 in mice results in a 75% reduction in the osmotic water permeability

of the inner medullary collecting duct (IMCD), 48-h fluid restriction in rats did not affect IM AQP4 [12,77]. In contrary to former beliefs, AQP4 has been shown to be in part AVP-sensitive [78]. Van Hoek et. al. demonstrated that AQP4 subtype abundance could be increased by V2R in a PKA dependent manner [79]. Studies in brain and retina have indicated that AVP and RAS hormones could play an important role by increasing AQP4 abundance under certain pathophysiological conditions [78,80]. Consistently, AQP4 was increased in L-Sham+d, HF, L-HF, and L-Sham vs. Sham. These results indicate that ANG II also takes part in AQP4 regulation in the kidney. Water retention in combination with decreased GFR and severe hyponatremia in nephrotic syndrome and liver cirrhosis have been associated with downregulation of AQP4 [81–83]. L-HF+d rats, who exhibited the most severe hyponatremia and a major decrease in Ccr, correspond with these findings. Indeed, short-term liver cirrhosis studies have revealed that decreased AQP2 expression is possible in the presence of hyponatremia, hypoosmolality, and sustained elevated AVP [83–85]. Thus, in certain settings of extracellular fluid volume expansion, excessive water retention with hyponatremia can occur in the absence of increased AQP2 abundance. Terris et al. suggested that the underlying mechanism was different from that in AVP-escape, because AVP-escape only affects AQP2 abundance but not AQP3 and AQP4, and our present findings support this hypothesis [13,83]. However, we cannot fully explain the observed differences in AQP4 abundance from L-Sham+d and L-HF+d in this study. McCoy and coworkers demonstrated that AQP4 facilitated water permeability is regulated by protein kinase C (PKC) raising the question whether circulating ANG II through AT1R could be modulating AQP4 through AT1R-V2R crosstalk, despite of downregulated AT1R [9,55,86,87].

AQP1 is downregulated in sodium restricted sham rats independently of DDAVP

The IMCD paracellular environment is highly hyperosmotic due to the reuptake and up-concentration of urea in this zone in conjunction with the thick ascending limbs, thereby enabling fine-tune urine concentration in the IMCD. This makes the inner medulla a focus for water retention states such as HF. Consistent with previous results in chronic-stage HF, AQP1, AQP3 and Na-K-ATPase were unaffected in HF vs. Sham [11]. Also, sodium restriction and DDAVP infusion did not affect AQP1 abundance among the HF group. In contrast, L-Sham and L-Sham+d downregulated IM AQP1 vs. Sham and L-HF rats. Decreased AQP1 in cortex and the inner stripe of outer medulla in sodium restricted rats co-treated with DDAVP and candesartan has previously been shown by our group [8]. It was suggested that AQP1 downregulation in these parts of the kidney could be due to either direct AT1R blockade or decreased GFR. In the present study, AT1R abundance was unaffected among sham groups (Fig. 6, E) and GFR (shown by Ccr) in L-Sham and Sham was unchanged. AQP1 alterations were confined to the sham groups only (Fig. 8, A, B, D, E). These observations make changes in GFR or AT1R as the prime effector less likely. Previous studies have demonstrated that AQP1 can be upregulated by elevated osmolality in kidney IM [88,89]. Urea, along with sodium chloride, constitutes a large portion of the medullary hyperosmolar driving force for water transport. U/P osmolality ratio increased in all animals receiving low sodium diet. Low sodium delivery to the loop of Henle and distal collecting ducts in combination with increased urea excretion could then lead to decreased medullary osmolality. These events could explain why AQP1 was decreased in L-Sham and L-Sham+d but they do not explain why AQP1 abundance in L-HF and L-HF+d was unaffected. The increased plasma urea in L-HF vs. L-Sham indicates that enhanced AVP-mediated urea reabsorption takes place in the terminal part of IMCD in HF. Hence, reduced IM

osmolality as indicated by increased urea washout could be responsible for decreased AQP1 in L-Sham and L-Sham+d vs. Sham ([Table 3](#)) [[43,90,91](#)].

Study limitations and clinical perspectives

The changes in protein abundance from the immunoblots in this study can seem relatively modest. However, the presented changes are within the range previously published using the same model [[9,45,46](#)]. In our experience, rats are resilient animals capable of surviving remarkably large infarcts with only modest changes in cardiac pumping ability and renal water and sodium retention, when compared to humans. Nevertheless, previous findings in HF rats have been confirmed in human studies [[5,92,93](#)]. We believe that our results are clinically important. They suggest that the kidney may possess intrinsic protecting factors against chronically elevated AVP during cardiac remodeling after MI, shown by partly blunted AQP2 recruitment. Blunted AQP2 recruitment has not previously been described in HF. Our results indicate that inhibition of AT1R synthesis is responsible. In the kidney, chronically RAS activation can lead to medullary necrosis, renal fibrosis, and chronic kidney failure [[94](#)]. Similar findings have been observed in the heart [[95,96](#)]. Further studies need to be performed to investigate whether targeted drug regimens can sustain or even enhance the beneficial compensation mechanism by the kidney seen in early-stage HF into later stages of HF. Finding the underlying reason why this protection seems to be stopping with finalization of cardiac remodeling needs to be further investigated and could have beneficial implication on the future clinical therapy post-MI. This could potentially lead to suppression of the vicious cycle of HF and/or decrease the levels of side effects in drug therapy such as drug induced hyponatremia.

Summary and Conclusion

Early-stage HF rats developed hyponatremia, hypo-osmolality, and decreased Ccr, but exhibited comparable IM AQP2 and p-AQP2 abundance to sham groups, despite of increased V2R abundance and marked apical staining of AQP2 shown by immunocytochemistry. Decreased type-1_A angiotensin II receptor abundances in all HF groups likely play a role in the transduction of these effects. (P)RR in the HF groups altered independently of V2R and AT1R abundance. AQP4 was decreased in L-HF rats but increased in sodium restricted Sham when chronically infused with DDAVP. Sodium restriction elicited decreased AQP1 abundance in Sham rats, but not in HF rats. We suggest that during early-stage HF the kidney may possess intrinsic protecting features against chronically elevated AVP and sustained increased AQP2 abundance. In conclusion, this study supports the importance of V2R-AT1R crosstalk in the development of HF.

Acknowledgments

We thank Helle Høyer, Gitte Kall, Gitte Skou, and Line Nielsen for expert technical assistance and Professor Erik Sloth, Department of Anaesthesia and Intensive Care, Aarhus University Hospital –Skejby, Denmark, for providing echocardiographic equipment and expertise.

Author Contributions

Conceived and designed the experiments: SCL JF SN. Performed the experiments: SCL. Analyzed the data: SCL JF SN. Contributed reagents/materials/analysis tools: SCL JF SN. Wrote the paper: SCL. Obtained approval of animal protocols: SCL JF. Raised specific antibodies or obtained permission for use of noncommercial antibodies: SN JF. Provided research of animal facilities: JF. Provided for expert labtech assistance: SN JF.

References

- Kim JK, Michel JB, Soubrier F, Durr J, Corvol P, et al. (1990) Arginine vasopressin gene expression in chronic cardiac failure in rats. *Kidney Int* 38: 818–822. PMID: [2266664](#)
- Xu DL, Martin PY, Ohara M, St John J, Pattison T, et al. (1997) Upregulation of aquaporin-2 water channel expression in chronic heart failure rat. *J Clin Invest* 99: 1500–1505. PMID: [9119993](#)
- Wong NL, Tsui JK (2002) Upregulation of vasopressin V2 and aquaporin 2 in the inner medullary collecting duct of cardiomyopathic hamsters is attenuated by enalapril treatment. *Metabolism* 51: 970–975. PMID: [12145768](#)
- Veeraveedu PT, Watanabe K, Ma M, Palaniyandi SS, Yamaguchi K, et al. (2007) Effects of nonpeptide vasopressin V2 antagonist tolvaptan in rats with heart failure. *Biochem Pharmacol* 74: 1466–1475. S0006-2952(07)00498-4 [pii]; doi: [10.1016/j.bcp.2007.07.027](#) PMID: [17720144](#)
- Pedersen RS, Bentzen H, Bech JN, Nyvad O, Pedersen EB (2003) Urinary aquaporin-2 in healthy humans and patients with liver cirrhosis and chronic heart failure during baseline conditions and after acute water load. *Kidney Int* 63: 1417–1425. PMID: [12631357](#)
- Oren RM (2005) Hyponatremia in congestive heart failure. *Am J Cardiol* 95: 2B–7B. S0002-9149(05)00353-X [pii]; doi: [10.1016/j.amjcard.2005.03.002](#) PMID: [15847851](#)
- Yu CM, Wing-Hon LK, Li PS, Lam KY, Leung JC, et al. (2004) Normalization of renal aquaporin-2 water channel expression by foscipril, valsartan, and combination therapy in congestive heart failure: a new mechanism of action. *J Mol Cell Cardiol* 36: 445–453. PMID: [15010283](#)
- Kwon TH, Nielsen J, Knepper MA, Frokiaer J, Nielsen S (2005) Angiotensin II AT1 receptor blockade decreases vasopressin-induced water reabsorption and AQP2 levels in NaCl-restricted rats. *Am J Physiol Renal Physiol* 288: F673–F684. PMID: [15585668](#)
- Lutken SC, Kim SW, Jonassen T, Marples D, Knepper MA, et al. (2009) Changes of renal AQP2, ENaC, and NHE3 in experimentally induced heart failure: response to angiotensin II AT1 receptor blockade. *Am J Physiol Renal Physiol* 297: F1678–F1688. 00010.2009 [pii]; doi: [10.1152/ajprenal.00010.2009](#) PMID: [19776175](#)
- Klingler C, Ancellin N, Barrault MB, Morel A, Buhler JM, et al. (1998) Angiotensin II potentiates vasopressin-dependent cAMP accumulation in CHO transfected cells. Mechanisms of cross-talk between AT1A and V2 receptors. *Cell Signal* 10: 65–74. PMID: [9502119](#)
- Nielsen S, Terris J, Andersen D, Ecelbarger C, Frokiaer J, et al. (1997) Congestive heart failure in rats is associated with increased expression and targeting of aquaporin-2 water channel in collecting duct. *Proc Natl Acad Sci U S A* 94: 5450–5455. PMID: [9144258](#)
- Terris J, Ecelbarger CA, Nielsen S, Knepper MA (1996) Long-term regulation of four renal aquaporins in rats. *Am J Physiol* 271: F414–F422. PMID: [8770174](#)
- Ecelbarger CA, Nielsen S, Olson BR, Murase T, Baker EA, et al. (1997) Role of renal aquaporins in escape from vasopressin-induced antidiuresis in rat. *J Clin Invest* 99: 1852–1863. PMID: [9109429](#)
- Johns TNP, Olson BJ (1954) Experimental Myocardial Infarction; a method of coronary occlusion in small animals. *Annals of Surgery* 140: 675–682. PMID: [13208115](#)
- Fishbein MC, Maclean D, Maroko PR (1978) Experimental myocardial infarction in the rat: qualitative and quantitative changes during pathologic evolution. *Am J Pathol* 90: 57–70. PMID: [619696](#)
- Pfeffer MA, Pfeffer JM, Fishbein MC, Fletcher PJ, Spadaro J, et al. (1979) Myocardial infarct size and ventricular function in rats. *Circ Res* 44: 503–512. PMID: [428047](#)
- Van de Werf F, Ardissino D, Betriu A, Cokkinos DV, Falk E, et al. (2003) Management of acute myocardial infarction in patients presenting with ST-segment elevation. The Task Force on the Management of Acute Myocardial Infarction of the European Society of Cardiology. *Eur Heart J* 24: 28–66. S0195668X02006188 [pii]. PMID: [12559937](#)
- Shao W, Seth DM, Prieto MC, Kobori H, Navar LG (2013) Activation of the renin-angiotensin system by a low-salt diet does not augment intratubular angiotensinogen and angiotensin II in rats. *Am J Physiol Renal Physiol* 304: F505–F514. ajprenal.00587.2012 [pii]; doi: [10.1152/ajprenal.00587.2012](#) PMID: [23303412](#)
- Schiller NB, Shah PM, Crawford M, DeMaria A, Devereux R, et al. (1989) Recommendations for quantitation of the left ventricle by two-dimensional echocardiography. American Society of Echocardiography Committee on Standards, Subcommittee on Quantitation of Two-Dimensional Echocardiograms. *J Am Soc Echocardiogr* 2: 358–367. PMID: [2698218](#)
- Lang RM, Bierig M, Devereux RB, Flachskampf FA, Foster E, et al. (2005) Recommendations for chamber quantification: a report from the American Society of Echocardiography's Guidelines and Standards Committee and the Chamber Quantification Writing Group, developed in conjunction with the European Association of Echocardiography, a branch of the European Society of Cardiology. *J Am Soc Echocardiogr* 18: 1440–1463. S0894-7317(05)00983-1 [pii]; doi: [10.1016/j.echo.2005.10.005](#) PMID: [16376782](#)

21. Wyatt HL, Meerbaum S, Heng MK, Gueret P, Corday E (1980) Cross-sectional echocardiography. III. Analysis of mathematic models for quantifying volume of symmetric and asymmetric left ventricles. *Am Heart J* 100: 821–828. PMID: [7446384](#)
22. Wasmeier GH, Melnychenko I, Voigt JU, Zimmermann WH, Eschenhagen T, et al. (2007) Reproducibility of transthoracic echocardiography in small animals using clinical equipment. *Coron Artery Dis* 18: 283–291. 00019501-200706000-00007 [pii]. doi: [10.1097/MCA.0b013e3280d5a7e3](#) PMID: [17496492](#)
23. Rose BD (1986) New approach to disturbances in the plasma sodium concentration. *Am J Med* 81: 1033–1040. 0002-9343(86)90401-8 [pii]. PMID: [3799631](#)
24. Goldberg M (1981) Hyponatremia. *Med Clin North Am* 65: 251–269. PMID: [7230957](#)
25. Kim SW, Wang W, Nielsen J, Praetorius J, Kwon TH, et al. (2004) Increased expression and apical targeting of renal ENaC subunits in puromycin aminonucleoside-induced nephrotic syndrome in rats. *Am J Physiol Renal Physiol* 286: F922–F935. PMID: [15075188](#)
26. Nielsen J, Kwon TH, Praetorius J, Kim YH, Frokiaer J, et al. (2003) Segment-specific ENaC downregulation in kidney of rats with lithium-induced NDI. *Am J Physiol Renal Physiol* 285: F1198–F1209. 00118.2003 [pii]. doi: [10.1152/ajprenal.00118.2003](#) PMID: [12928314](#)
27. Brooks HL, Sorensen AM, Terris J, Schultheis PJ, Lorenz JN, et al. (2001) Profiling of renal tubule Na⁺ transporter abundances in NHE3 and NCC null mice using targeted proteomics. *J Physiol* 530: 359–366. PMID: [11158268](#)
28. Schneider CA, Rasband WS, Eliceiri KW (2012) NIH Image to ImageJ: 25 years of image analysis. *Nat Methods* 9: 671–675. PMID: [22930834](#)
29. Nielsen J, Kwon TH, Praetorius J, Frokiaer J, Knepper MA, et al. (2006) Aldosterone increases urine production and decreases apical AQP2 expression in rats with diabetes insipidus. *Am J Physiol Renal Physiol* 290: F438–F449. 00158.2005 [pii]; doi: [10.1152/ajprenal.00158.2005](#) PMID: [16159898](#)
30. Christensen BM, Zelenina M, Aperia A, Nielsen S (2000) Localization and regulation of PKA-phosphorylated AQP2 in response to V(2)-receptor agonist/antagonist treatment. *Am J Physiol Renal Physiol* 278: F29–F42. PMID: [10644653](#)
31. Jensen AM, Bae EH, Fenton RA, Norregaard R, Nielsen S, et al. (2009) Angiotensin II regulates V2 receptor and pAQP2 during ureteral obstruction. *Am J Physiol Renal Physiol* 296: F127–F134. 90479.2008 [pii]; doi: [10.1152/ajprenal.90479.2008](#) PMID: [18971210](#)
32. Fenton RA, Brond L, Nielsen S, Praetorius J (2007) Cellular and subcellular distribution of the type-2 vasopressin receptor in the kidney. *Am J Physiol Renal Physiol* 293: F748–F760. 00316.2006 [pii]; doi: [10.1152/ajprenal.00316.2006](#) PMID: [17553938](#)
33. Kwon TH, Nielsen J, Masilamani S, Hager H, Knepper MA, et al. (2002) Regulation of collecting duct AQP3 expression: response to mineralocorticoid. *Am J Physiol Renal Physiol* 283: F1403–F1421. PMID: [12388415](#)
34. O'Neill H, Lebeck J, Collins PB, Kwon TH, Frokiaer J, et al. (2008) Aldosterone-mediated apical targeting of ENaC subunits is blunted in rats with streptozotocin-induced diabetes mellitus. *Nephrol Dial Transplant* 23: 1546–1555. gfm814 [pii]; doi: [10.1093/ndt/gfm814](#) PMID: [18029369](#)
35. Nielsen S, Smith BL, Christensen EI, Knepper MA, Agre P (1993) CHIP28 water channels are localized in constitutively water-permeable segments of the nephron. *J Cell Biol* 120: 371–383. PMID: [7678419](#)
36. Kwon TH, Nielsen J, Kim YH, Knepper MA, Frokiaer J, et al. (2003) Regulation of sodium transporters in the thick ascending limb of rat kidney: response to angiotensin II. *Am J Physiol Renal Physiol* 285: F152–F165. PMID: [12657563](#)
37. Kamsteeg EJ, Heijnen I, van Os CH, Deen PM (2000) The subcellular localization of an aquaporin-2 tetramer depends on the stoichiometry of phosphorylated and nonphosphorylated monomers. *J Cell Biol* 151: 919–930. PMID: [11076974](#)
38. Christensen BM, Wang W, Frokiaer J, Nielsen S (2003) Axial heterogeneity in basolateral AQP2 localization in rat kidney: effect of vasopressin. *Am J Physiol Renal Physiol* 284: F701–F717. PMID: [12453871](#)
39. Nguyen G (2006) Renin/prorenin receptors. *Kidney Int* 69: 1503–1506. 5000265 [pii]; doi: [10.1038/sj.ki.5000265](#) PMID: [16672920](#)
40. Ecelbarger CA, Terris J, Frindt G, Echevarria M, Marples D, et al. (1995) Aquaporin-3 water channel localization and regulation in rat kidney. *Am J Physiol* 269: F663–F672. PMID: [7503232](#)
41. Kim SW, Gresz V, Rojek A, Wang W, Verkman AS, et al. (2005) Decreased expression of AQP2 and AQP4 water channels and Na,K-ATPase in kidney collecting duct in AQP3 null mice. *Biol Cell* 97: 765–778. PMID: [15898956](#)
42. Zhai XY, Fenton RA, Andreassen A, Thomsen JS, Christensen EI (2007) Aquaporin-1 is not expressed in descending thin limbs of short-loop nephrons. *J Am Soc Nephrol* 18: 2937–2944. ASN.2007010056 [pii]; doi: [10.1681/ASN.2007010056](#) PMID: [17942963](#)

43. Lanaspá MA, Andres-Hernando A, Li N, Rivard CJ, Cicerchi C, et al. (2010) The expression of aquaporin-1 in the medulla of the kidney is dependent on the transcription factor associated with hypertonicity, TonEBP. *J Biol Chem* 285: 31694–31703. M109.093690 [pii]; doi: [10.1074/jbc.M109.093690](https://doi.org/10.1074/jbc.M109.093690) PMID: [20639513](https://pubmed.ncbi.nlm.nih.gov/20639513/)
44. Ma T, Frigeri A, Hasegawa H, Verkman AS (1994) Cloning of a water channel homolog expressed in brain meningeal cells and kidney collecting duct that functions as a stilbene-sensitive glycerol transporter. *J Biol Chem* 269: 21845–21849. PMID: [8063828](https://pubmed.ncbi.nlm.nih.gov/8063828/)
45. Staahltoft D, Nielsen S, Janjua NR, Christensen S, Skott O, et al. (2002) Losartan treatment normalizes renal sodium and water handling in rats with mild congestive heart failure. *Am J Physiol Renal Physiol* 282: F307–F315. PMID: [11788445](https://pubmed.ncbi.nlm.nih.gov/11788445/)
46. Brond L, Mullertz KM, Torp M, Nielsen J, Graebe M, et al. (2013) Congestive heart failure in rats is associated with increased collecting duct vasopressin sensitivity and vasopressin type 2 receptor reexternalization. *Am J Physiol Renal Physiol* 305: F1547–F1554. *ajprenal.00461.2012* [pii]; doi: [10.1152/ajprenal.00461.2012](https://doi.org/10.1152/ajprenal.00461.2012) PMID: [24089411](https://pubmed.ncbi.nlm.nih.gov/24089411/)
47. Marples D, Christensen BM, Frokiaer J, Knepper MA, Nielsen S (1998) Dehydration reverses vasopressin antagonist-induced diuresis and aquaporin-2 downregulation in rats. *Am J Physiol* 275: F400–F409. PMID: [9729513](https://pubmed.ncbi.nlm.nih.gov/9729513/)
48. Marples D, Knepper MA, Christensen EI, Nielsen S (1995) Redistribution of aquaporin-2 water channels induced by vasopressin in rat kidney inner medullary collecting duct. *Am J Physiol* 269: C655–C664. PMID: [7573395](https://pubmed.ncbi.nlm.nih.gov/7573395/)
49. Stegbauer J, Gurley SB, Sparks MA, Woznowski M, Kohan DE, et al. (2011) AT1 receptors in the collecting duct directly modulate the concentration of urine. *J Am Soc Nephrol* 22: 2237–2246. ASN.2010101095 [pii]; doi: [10.1681/ASN.2010101095](https://doi.org/10.1681/ASN.2010101095) PMID: [22052052](https://pubmed.ncbi.nlm.nih.gov/22052052/)
50. Maeda Y, Han JS, Gibson CC, Knepper MA (1993) Vasopressin and oxytocin receptors coupled to Ca²⁺ mobilization in rat inner medullary collecting duct. *Am J Physiol* 265: F15–F25. PMID: [8393622](https://pubmed.ncbi.nlm.nih.gov/8393622/)
51. Champigneulle A, Siga E, Vassent G, Imbert-Teboul M (1993) V2-like vasopressin receptor mobilizes intracellular Ca²⁺ in rat medullary collecting tubules. *Am J Physiol* 265: F35–F45. PMID: [8342613](https://pubmed.ncbi.nlm.nih.gov/8342613/)
52. Ecelbarger CA, Chou CL, Lolait SJ, Knepper MA, DiGiovanni SR (1996) Evidence for dual signaling pathways for V2 vasopressin receptor in rat inner medullary collecting duct. *Am J Physiol* 270: F623–F633. PMID: [8967340](https://pubmed.ncbi.nlm.nih.gov/8967340/)
53. Star RA, Nonoguchi H, Balaban R, Knepper MA (1988) Calcium and cyclic adenosine monophosphate as second messengers for vasopressin in the rat inner medullary collecting duct. *J Clin Invest* 81: 1879–1888. PMID: [2838523](https://pubmed.ncbi.nlm.nih.gov/2838523/)
54. Chou CL, Yip KP, Michea L, Kador K, Ferraris JD, et al. (2000) Regulation of aquaporin-2 trafficking by vasopressin in the renal collecting duct. Roles of ryanodine-sensitive Ca²⁺ stores and calmodulin. *J Biol Chem* 275: 36839–36846. PMID: [10973964](https://pubmed.ncbi.nlm.nih.gov/10973964/)
55. Lee YJ, Song IK, Jang KJ, Nielsen J, Frokiaer J, et al. (2007) Increased AQP2 targeting in primary cultured IMCD cells in response to angiotensin II through AT1 receptor. *Am J Physiol Renal Physiol* 292: F340–F350. 00090.2006 [pii]; doi: [10.1152/ajprenal.00090.2006](https://doi.org/10.1152/ajprenal.00090.2006) PMID: [16896188](https://pubmed.ncbi.nlm.nih.gov/16896188/)
56. Yip KP (2006) Epac-mediated Ca(2+) mobilization and exocytosis in inner medullary collecting duct. *Am J Physiol Renal Physiol* 291: F882–F890. 00411.2005 [pii]; doi: [10.1152/ajprenal.00411.2005](https://doi.org/10.1152/ajprenal.00411.2005) PMID: [16684923](https://pubmed.ncbi.nlm.nih.gov/16684923/)
57. Bos JL (2003) Epac: a new cAMP target and new avenues in cAMP research. *Nat Rev Mol Cell Biol* 4: 733–738. nrm1197 [pii]. doi: [10.1038/nrm1197](https://doi.org/10.1038/nrm1197) PMID: [14506476](https://pubmed.ncbi.nlm.nih.gov/14506476/)
58. Bouby N, Hus-Citharel A, Marchetti J, Bankir L, Corvol P, et al. (1997) Expression of type 1 angiotensin II receptor subtypes and angiotensin II-induced calcium mobilization along the rat nephron. *J Am Soc Nephrol* 8: 1658–1667. PMID: [9355068](https://pubmed.ncbi.nlm.nih.gov/9355068/)
59. Poggioli J, Lazar G, Houillier P, Gardin JP, Achard JM, et al. (1992) Effects of angiotensin II and non-peptide receptor antagonists on transduction pathways in rat proximal tubule. *Am J Physiol* 263: C750–C758. PMID: [1329542](https://pubmed.ncbi.nlm.nih.gov/1329542/)
60. Bustamante M, Hasler U, Kotova O, Chibalin AV, Mordasini D, et al. (2005) Insulin potentiates AVP-induced AQP2 expression in cultured renal collecting duct principal cells. *Am J Physiol Renal Physiol* 288: F334–F344. 00180.2004 [pii]; doi: [10.1152/ajprenal.00180.2004](https://doi.org/10.1152/ajprenal.00180.2004) PMID: [15494547](https://pubmed.ncbi.nlm.nih.gov/15494547/)
61. Ostrom RS, Naugle JE, Hase M, Gregorian C, Swaney JS, et al. (2003) Angiotensin II enhances adenylyl cyclase signaling via Ca²⁺/calmodulin. Gq-Gs cross-talk regulates collagen production in cardiac fibroblasts. *J Biol Chem* 278: 24461–24468. M212659200 [pii]. doi: [10.1074/jbc.M212659200](https://doi.org/10.1074/jbc.M212659200) PMID: [12711600](https://pubmed.ncbi.nlm.nih.gov/12711600/)

62. Nadler SP, Zimpelmann JA, Hebert RL (1992) Endothelin inhibits vasopressin-stimulated water permeability in rat terminal inner medullary collecting duct. *J Clin Invest* 90: 1458–1466. doi: [10.1172/JCI116013](https://doi.org/10.1172/JCI116013) PMID: [1328300](https://pubmed.ncbi.nlm.nih.gov/1328300/)
63. Kishore BK, Chou CL, Knepper MA (1995) Extracellular nucleotide receptor inhibits AVP-stimulated water permeability in inner medullary collecting duct. *Am J Physiol* 269: F863–F869. PMID: [8594881](https://pubmed.ncbi.nlm.nih.gov/8594881/)
64. van Balkom BW, Savelkoul PJ, Markovich D, Hofman E, Nielsen S, et al. (2002) The role of putative phosphorylation sites in the targeting and shuttling of the aquaporin-2 water channel. *J Biol Chem* 277: 41473–41479. PMID: [12194985](https://pubmed.ncbi.nlm.nih.gov/12194985/)
65. Kamsteeg EJ, Hendriks G, Boone M, Konings IB, Oorschot V, et al. (2006) Short-chain ubiquitination mediates the regulated endocytosis of the aquaporin-2 water channel. *Proc Natl Acad Sci U S A* 103: 18344–18349. 0604073103 [pii]; doi: [10.1073/pnas.0604073103](https://doi.org/10.1073/pnas.0604073103) PMID: [17101973](https://pubmed.ncbi.nlm.nih.gov/17101973/)
66. Tamma G, Procino G, Strafino A, Bononi E, Meyer G, Paulmichl M, et al. (2007) Hypotonicity induces aquaporin-2 internalization and cytosol-to-membrane translocation of ICln in renal cells. *Endocrinology* 148: 1118–1130. en.2006-1277 [pii]; doi: [10.1210/en.2006-1277](https://doi.org/10.1210/en.2006-1277) PMID: [17138647](https://pubmed.ncbi.nlm.nih.gov/17138647/)
67. Hasler U, Nunes P, Bouley R, Lu HA, Matsuzaki T, et al. (2008) Acute hypertonicity alters aquaporin-2 trafficking and induces a MAPK-dependent accumulation at the plasma membrane of renal epithelial cells. *J Biol Chem* 283: 26643–26661. M801071200 [pii]; doi: [10.1074/jbc.M801071200](https://doi.org/10.1074/jbc.M801071200) PMID: [18664568](https://pubmed.ncbi.nlm.nih.gov/18664568/)
68. van Balkom BW, van RM, Breton S, Pastor-Soler N, Bouley R, et al. (2003) Hypertonicity is involved in redirecting the aquaporin-2 water channel into the basolateral, instead of the apical, plasma membrane of renal epithelial cells. *J Biol Chem* 278: 1101–1107. M207339200 [pii]. doi: [10.1074/jbc.M207339200](https://doi.org/10.1074/jbc.M207339200) PMID: [12374804](https://pubmed.ncbi.nlm.nih.gov/12374804/)
69. Luk JK, Wong EF, Wong NL (1993) Hypersensitivity of inner medullary collecting duct cells to arginine vasopressin and forskolin in cardiomyopathic hamsters. *Cardiology* 83: 49–54. PMID: [8261487](https://pubmed.ncbi.nlm.nih.gov/8261487/)
70. Torp M, Brond L, Hadrup N, Nielsen JB, Praetorius J, et al. (2007) Losartan decreases vasopressin-mediated cAMP accumulation in the thick ascending limb of the loop of Henle in rats with congestive heart failure. *Acta Physiol (Oxf)* 190: 339–350. APS1722 [pii]; doi: [10.1111/j.1748-1716.2007.01722.x](https://doi.org/10.1111/j.1748-1716.2007.01722.x) PMID: [17635349](https://pubmed.ncbi.nlm.nih.gov/17635349/)
71. Ichikawa I, Pfeffer JM, Pfeffer MA, Hostetter TH, Brenner BM (1984) Role of angiotensin II in the altered renal function of congestive heart failure. *Circ Res* 55: 669–675. PMID: [6091942](https://pubmed.ncbi.nlm.nih.gov/6091942/)
72. Nguyen G, Delarue F, Burckle C, Bouzhir L, Giller T, et al. (2002) Pivotal role of the renin/prorenin receptor in angiotensin II production and cellular responses to renin. *J Clin Invest* 109: 1417–1427. doi: [10.1172/JCI14276](https://doi.org/10.1172/JCI14276) PMID: [12045255](https://pubmed.ncbi.nlm.nih.gov/12045255/)
73. Umenishi F, Nariakiyo T, Vandewalle A, Schrier RW (2006) cAMP regulates vasopressin-induced AQP2 expression via protein kinase A-independent pathway. *Biochim Biophys Acta* 1758: 1100–1105. S0005-2736(06)00211-2 [pii]; doi: [10.1016/j.bbame.2006.06.001](https://doi.org/10.1016/j.bbame.2006.06.001) PMID: [16844078](https://pubmed.ncbi.nlm.nih.gov/16844078/)
74. Takahashi K, Hiraishi K, Hirose T, Kato I, Yamamoto H, et al. (2010) Expression of (pro)renin receptor in the human brain and pituitary, and co-localisation with arginine vasopressin and oxytocin in the hypothalamus. *J Neuroendocrinol* 22: 453–459. JNE1980 [pii]; doi: [10.1111/j.1365-2826.2010.01980.x](https://doi.org/10.1111/j.1365-2826.2010.01980.x) PMID: [20163518](https://pubmed.ncbi.nlm.nih.gov/20163518/)
75. Contrepas A, Walker J, Koulakoff A, Franek KJ, Qadri F, et al. (2009) A role of the (pro)renin receptor in neuronal cell differentiation. *Am J Physiol Regul Integr Comp Physiol* 297: R250–R257. 90832.2008 [pii]; doi: [10.1152/ajpregu.90832.2008](https://doi.org/10.1152/ajpregu.90832.2008) PMID: [19474391](https://pubmed.ncbi.nlm.nih.gov/19474391/)
76. Takahashi K, Yatabe M, Fujiwara K, Hirose T, Totsune K, et al. (2013) In Situ Hybridization Method Reveals (Pro)renin Receptor Expressing Cells in the Pituitary Gland of Rats: Correlation with Anterior Pituitary Hormones. *Acta Histochem Cytochem* 46: 47–50. AHC12030 [pii]. doi: [10.1267/ahc.12030](https://doi.org/10.1267/ahc.12030) PMID: [23554540](https://pubmed.ncbi.nlm.nih.gov/23554540/)
77. Chou CL, Ma T, Yang B, Knepper MA, Verkman AS (1998) Fourfold reduction of water permeability in inner medullary collecting duct of aquaporin-4 knockout mice. *Am J Physiol* 274: C549–C554. PMID: [9486146](https://pubmed.ncbi.nlm.nih.gov/9486146/)
78. Moeller HB, Fenton RA, Zeuthen T, Macaulay N (2009) Vasopressin-dependent short-term regulation of aquaporin 4 expressed in *Xenopus* oocytes. *Neuroscience* 164: 1674–1684. S0306-4522(09)01630-3 [pii]; doi: [10.1016/j.neuroscience.2009.09.072](https://doi.org/10.1016/j.neuroscience.2009.09.072) PMID: [19800950](https://pubmed.ncbi.nlm.nih.gov/19800950/)
79. Van Hoek AN, Bouley R, Lu Y, Silberstein C, Brown D, et al. (2009) Vasopressin-induced differential stimulation of AQP4 splice variants regulates the in-membrane assembly of orthogonal arrays. *Am J Physiol Renal Physiol* 296: F1396–F1404. 00018.2009 [pii]; doi: [10.1152/ajprenal.00018.2009](https://doi.org/10.1152/ajprenal.00018.2009) PMID: [19297454](https://pubmed.ncbi.nlm.nih.gov/19297454/)
80. Qin Y, Ren H, Hoffman MR, Fan J, Zhang M, et al. (2012) Aquaporin changes during diabetic retinopathy in rats are accelerated by systemic hypertension and are linked to the renin-angiotensin system.

- Invest Ophthalmol Vis Sci 53: 3047–3053. iofs.11-9154 [pii]; doi: [10.1167/iovs.11-9154](https://doi.org/10.1167/iovs.11-9154) PMID: [22491408](https://pubmed.ncbi.nlm.nih.gov/22491408/)
81. Apostol E, Ecelbarger CA, Terris J, Bradford AD, Andrews P, et al. (1997) Reduced renal medullary water channel expression in puromycin aminonucleoside—induced nephrotic syndrome. *J Am Soc Nephrol* 8: 15–24. PMID: [9013444](https://pubmed.ncbi.nlm.nih.gov/9013444/)
82. Kim SW, Cho SH, Oh BS, Yeum CH, Choi KC, et al. (2001) Diminished renal expression of aquaporin water channels in rats with experimental bilateral ureteral obstruction. *J Am Soc Nephrol* 12: 2019–2028. PMID: [11562400](https://pubmed.ncbi.nlm.nih.gov/11562400/)
83. Fernandez-Llama P, Turner R, Dibona G, Knepper MA (1999) Renal expression of aquaporins in liver cirrhosis induced by chronic common bile duct ligation in rats. *J Am Soc Nephrol* 10: 1950–1957. PMID: [10477147](https://pubmed.ncbi.nlm.nih.gov/10477147/)
84. Jonassen TE, Nielsen S, Christensen S, Petersen JS (1998) Decreased vasopressin-mediated renal water reabsorption in rats with compensated liver cirrhosis. *Am J Physiol* 275: F216–F225. PMID: [9691010](https://pubmed.ncbi.nlm.nih.gov/9691010/)
85. Jonassen TE, Christensen S, Kwon TH, Langhoff S, Salling N, et al. (2000) Renal water handling in rats with decompensated liver cirrhosis. *Am J Physiol Renal Physiol* 279: F1101–F1109. PMID: [11097629](https://pubmed.ncbi.nlm.nih.gov/11097629/)
86. McCoy ES, Haas BR, Sontheimer H (2010) Water permeability through aquaporin-4 is regulated by protein kinase C and becomes rate-limiting for glioma invasion. *Neuroscience* 168: 971–981. S0306-4522 (09)01495-X [pii]; doi: [10.1016/j.neuroscience.2009.09.020](https://doi.org/10.1016/j.neuroscience.2009.09.020) PMID: [19761816](https://pubmed.ncbi.nlm.nih.gov/19761816/)
87. Puri PL, Avantaggiati ML, Burgio VL, Chirillo P, Colleparado D, et al. (1995) Reactive oxygen intermediates mediate angiotensin II-induced c-Jun.c-Fos heterodimer DNA binding activity and proliferative hypertrophic responses in myogenic cells. *J Biol Chem* 270: 22129–22134. PMID: [7673190](https://pubmed.ncbi.nlm.nih.gov/7673190/)
88. Umenishi F, Yoshihara S, Narikiyo T, Schrier RW (2005) Modulation of hypertonicity-induced aquaporin-1 by sodium chloride, urea, betaine, and heat shock in murine renal medullary cells. *J Am Soc Nephrol* 16: 600–607. ASN.2004030241 [pii]; doi: [10.1681/ASN.2004030241](https://doi.org/10.1681/ASN.2004030241) PMID: [15647343](https://pubmed.ncbi.nlm.nih.gov/15647343/)
89. Umenishi F, Schrier RW (2003) Hypertonicity-induced aquaporin-1 (AQP1) expression is mediated by the activation of MAPK pathways and hypertonicity-responsive element in the AQP1 gene. *J Biol Chem* 278: 15765–15770. M209980200 [pii]. doi: [10.1074/jbc.M209980200](https://doi.org/10.1074/jbc.M209980200) PMID: [12600999](https://pubmed.ncbi.nlm.nih.gov/12600999/)
90. Sands JM, Nonoguchi H, Knepper MA (1987) Vasopressin effects on urea and H₂O transport in inner medullary collecting duct subsegments. *Am J Physiol* 253: F823–F832. PMID: [3688238](https://pubmed.ncbi.nlm.nih.gov/3688238/)
91. Fenton RA (2009) Essential role of vasopressin-regulated urea transport processes in the mammalian kidney. *Pflugers Arch* 458: 169–177. doi: [10.1007/s00424-008-0612-4](https://doi.org/10.1007/s00424-008-0612-4) PMID: [19011892](https://pubmed.ncbi.nlm.nih.gov/19011892/)
92. Funayama H, Nakamura T, Saito T, Yoshimura A, Saito M, et al. (2004) Urinary excretion of aquaporin-2 water channel exaggerated dependent upon vasopressin in congestive heart failure. *Kidney Int* 66: 1387–1392. KID902 [pii]. doi: [10.1111/j.1523-1755.2004.00902.x](https://doi.org/10.1111/j.1523-1755.2004.00902.x) PMID: [15458431](https://pubmed.ncbi.nlm.nih.gov/15458431/)
93. Biner HL, Arpin-Bott MP, Loffing J, Wang X, Knepper M, et al. (2002) Human cortical distal nephron: distribution of electrolyte and water transport pathways. *J Am Soc Nephrol* 13: 836–847. PMID: [11912242](https://pubmed.ncbi.nlm.nih.gov/11912242/)
94. Gilbert RE, Wu LL, Kelly DJ, Cox A, Wilkinson-Berka JL, et al. (1999) Pathological expression of renin and angiotensin II in the renal tubule after subtotal nephrectomy. Implications for the pathogenesis of tubulointerstitial fibrosis. *Am J Pathol* 155: 429–440. S0002-9440(10)65139-5 [pii]; doi: [10.1016/S0002-9440\(10\)65139-5](https://doi.org/10.1016/S0002-9440(10)65139-5) PMID: [10433936](https://pubmed.ncbi.nlm.nih.gov/10433936/)
95. Yamazaki T, Komuro I, Yazaki Y (1999) Role of the renin-angiotensin system in cardiac hypertrophy. *Am J Cardiol* 83: 53H–57H. PMID: [10750588](https://pubmed.ncbi.nlm.nih.gov/10750588/)
96. Patrucco E, Domes K, Sbroglio M, Blaich A, Schlossmann J, et al. (2014) Roles of cGMP-dependent protein kinase I (cGKI) and PDE5 in the regulation of Ang II-induced cardiac hypertrophy and fibrosis. *Proc Natl Acad Sci U S A* 111: 12925–12929. 1414364111 [pii]; doi: [10.1073/pnas.1414364111](https://doi.org/10.1073/pnas.1414364111) PMID: [25139994](https://pubmed.ncbi.nlm.nih.gov/25139994/)